Systems and Control Group

Thesis Systems and Control

Concentration based flow control in acoustic separation of suspensions

Lyubka Stefanova

March 2012

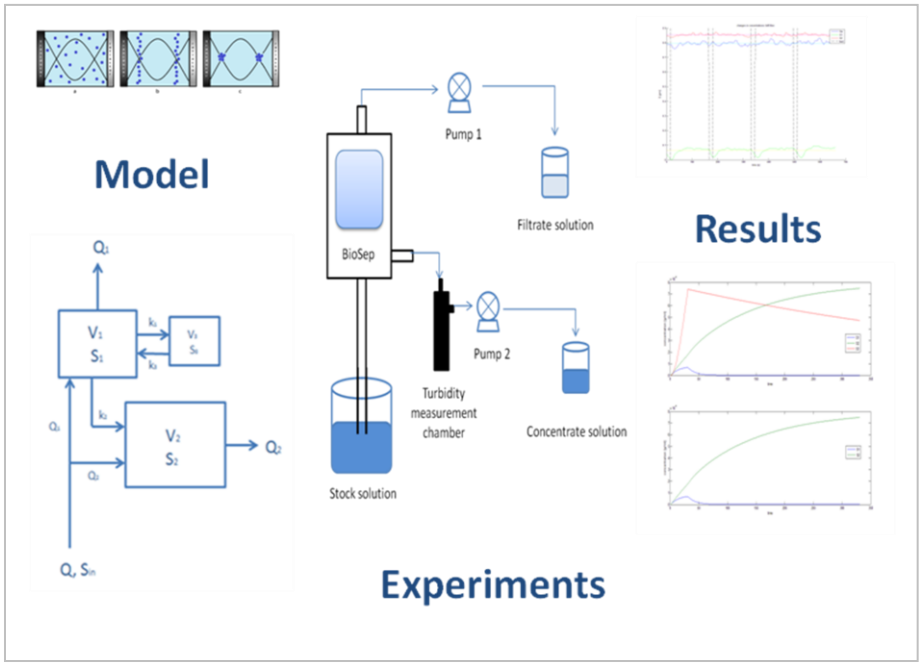

WAGENINGEN UNIVERSITY
AGROTECHNOLOGY AND
FOOD SCIENCES

Concentration based flow control in acoustic separation of suspensions

Name course	:	Thesis project Systems and Control
Number	:	SCO-80439
Study load	:	39 ECTS
Date	:	March 2012

Student	:	Lyubka Antobova Stefanova
Registration number	:	871111-800-130
Study programme	:	MBT (Biotechnology)
Supervisor(s)	:	Dr. ir. K. J. Keesman
		Ir. H. Cappon
Examiner	:	Dr. ir. L.G. van Willigenburg
Group	:	Systems and Control Group
Address	:	Bornse Weilanden 9
		Building 118
		6708 WG Wageningen
		The Netherlands
		Tel: +31 (317) 48 21 24

Contents

Acknowledgements

I would like to express my special gratitude towards my supervisors Dr. ir. Karel Keesman and ir. Hans Cappon for their guidance, comments and constant support. I would like to thank Karel Keesman especially for the discussions, for the invaluable assistance, with which he provided me for my computer programming and Matlab work and also for the endless patience. Thanks to Hans Cappon, who gave me interesting ideas for the experiments. I would also like to thanks to Ing. Kees van Asselt for his assistance for the dynamic data collection. Finally, I would like to thank all the students and stuff at the SCO Department, Wageningen University for the friendly environment and the nice time spent with them.

Abstract

Acoustic separation is a relatively new method for recovering valuable particulate matter from suspensions, which is mainly used in medical technology. However, this technique can also be applied for (waste) water treatment in order to clean the water. Moreover, this technique gives an opportunity to recover valuable constituents from the residual streams. As a result, the water is purified and the valuable constituents are recovered.

In the current study a commercially available device named BioSep, which employs so called 'ultrasound enhanced sedimentation' technique, is used to separate suspensions. In order to achieve certain quality of the water and certain level of constituents' recovery the BioSep should be controlled. A switching open-loop control strategy for this device, such that high separation efficiency can be achieved is designed using a numerical-experimental approach. Firstly, the BioSep is modeled and the system properties are studied. Then, the unknown parameters are estimated and subsequently, the values of the control input levels are determined.

List of symbols

Symbol	Definition	Units
S_{in}	concentration in the stock solution	g/ml
S_1	concentration in compartment 1	g/ml
S_2	concentration in compartment 2	g/ml
S_3	concentration in compartment 3	g/ml
V_1	volume of compartment 1	ml
V_2	volume of compartment 2	ml
V_3	volume of compartment 3	ml
Q_{in}	influent flow rate	ml/s
Q_1	filtrate flow rate	ml/s
Q_2	filtrate flow rate	ml/s
α	transducer coefficient	-
k_1	concentration coefficient ("rate constant" of the concentration reaction)	s^{-1}
k_2	settling coefficient ("rate constant" of the settling reaction)	ml/s^2
k_3	reverse concentration coefficient ("rate constant" of the reverse concentration reaction)	s^{-1}
k_4	loss coefficient (flow rate of "loses" from compartment 1 due to the turbulence flow)	ml/s

1. Introduction

Ismail Serageldin, Chairman of the World Commission on Water for the 21st Century said at Water Forum in The Netherlands on 30th of November, 1999:

“More than one-half of the world's major rivers are being seriously depleted and polluted, degrading and poisoning the surrounding ecosystems, thus threatening the health and livelihood of people who depend upon them for irrigation, drinking and industrial water.”

Even after more than 10 years, this quote depicts the main problem related to water, nowadays.

1.1. Problem definition

Nowadays, not only purifying the water is highly important, but also recovering the valuable constituents present in it. Therefore, both of these topics are taken into consideration. In the current study a device named BioSep, which employs so called ‘ultrasound enhanced sedimentation’ technique, is used for suspension separation. The possible application of this device for (waste) water treatment is tested. A quantity called separation efficiency is used for evaluation of the separation process. In order to achieve certain quality of the water and certain level of constituents’ recovery the BioSep should be controlled. Thus, the main problem of this study is how to control the BioSep to achieve high separation efficiency.

1.2. Objectives

The main objective of this study is to design a control strategy for the BioSep, such that high separation efficiency can be achieved. This objective implies system identification, which consists of modeling and parameters estimation.

1.3. Research questions

The objective discussed in the previous section results in the following research questions:

- How do the suspended particles behave during the separation process?
- How to model the system?
- What are the system properties?
- How to derive the unknown parameters in the model?
- How to properly design a switching open-loop control strategy?

1.4. Approach

In order to answer the research questions and to design the control strategy for the device a numerical-experimental approach is used. The first step of this approach is to model the system of interest, which in this case is BioSep. The system properties are examined in the next step. Afterwards, a steady state analysis is performed in order to see which of the unknown parameters from the model can be determined from the steady states. Then, experimental data are used for

estimations of the parameters. After that, the behaviour of the system is simulated using the estimated parameters. The final step is the design of switching open-loop control strategy.

1.5. Outline of the thesis

The thesis report starts with *Introduction* followed by the chapter *Theoretical background*, which gives the overview on solid-liquid separation, generation of ultrasonic fields and effects of the ultrasonic field on suspended particles. Ultrasound enhanced sedimentation and applications of ultrasonic field in solid-liquid separation are also reviewed in this chapter. After that all materials and methods, used during this study, are described in the third chapter called *Materials and Methods*. This chapter has two sections – *Modelling* and *Experiments*. The introduction of the BioSep's model, properties of the model and also a steady state analysis are given in the *Modelling* section. The next section, namely *Experiments,* gives description of the experiments and their setups. After that new chapter *Results and Discussion* follows. The results from the experiments, parameter estimation and the design for switching open-loop control strategy are presented and discussed in it. Moreover, simulations of the behaviour of the system when it is not controlled and when it is controlled are also included in the chapter *Results and Discussion. Conclusion* and *Recommendations* are the last two chapters of the report. In addition to these chapters, ten appendixes give supplementary information to the main text of the report.

2. Theoretical background

This chapter gives the theoretical overview on solid-liquid separation, generation of ultrasonic fields and effects of the ultrasonic field on suspended particles. Ultrasound enhanced sedimentation is also reviewed. Furthermore, applications of ultrasonic field in solid-liquid separation are briefly described.

2.1. Solid-liquid separation

Separation technology plays an important role in the process industries. Solid-liquid separation is a common type of separation used in most of the process industries in which particulate slurries are handled. By this separation solid and liquid components, which are constituents of every suspension, are separated. The solid-liquid separation allows 1) recycling and reusing of both phases of the suspension; 2) recovering and dewatering of the valuables solids (particles); 3) recovering and cleaning the liquid. Thus, the process becomes more efficient and environmentally friendly [1].

The methods used for solid-liquid separation can be divided into two categories depending on the type of separation process (see figure 1). The first category includes all conventional methods. The separation processes occupied in the conventional methods rely only on mechanical forces. Flotation, sedimentation, filtration, which are based on gravity force, are examples for conventional solid-liquid separation processes. However, when the separation processes are enhanced with energy supplied from an external force field the methods are called enhanced methods. Thus, they form the second category of solid-liquid separation methods. These methods have reduced reliance on mechanical force compared to the conventional methods due to the external force field, with which they are supplemented. As a result, the separation performance of the enhanced methods is improved in comparison to the conventional methods. In other words, greater recovery can be achieved with the enhanced solid-liquid separation methods than with the conventional ones [1, 2].

Further subdivision of the enhanced methods can be done according to the type of external force field (see figure 1). There are mainly three types of field - electric, sonic and magnetic, which can be applied. Field-assisted separation which combines different types of field is also possible [2]. The focus of this study is on the enhanced separation method using an ultrasonic field.

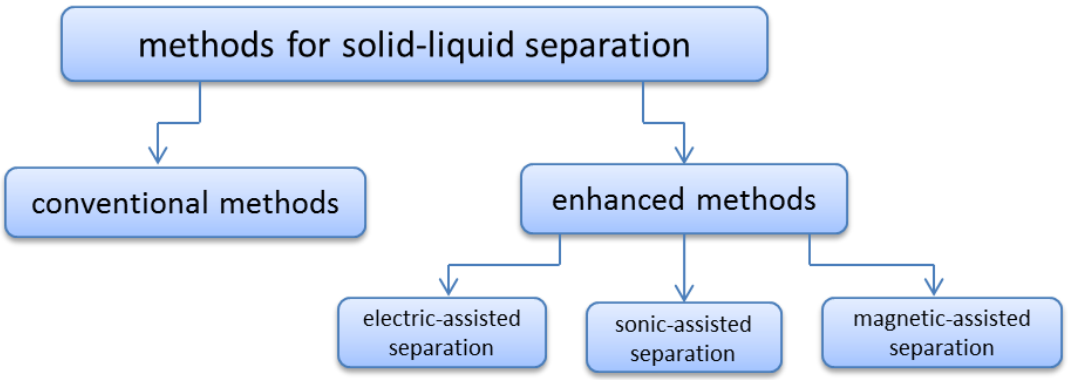

Figure 1 Classification of the methods used for solid-liquid separation

2.2. Ultrasonic field

In order to generate an ultrasonic field with standing waves a resonator is needed. A planar resonator typically consists of three main parts – transducer, reflector and carrier material. Usually these three components are arranged in layers. The space bounded between the reflector and carrier material is for the fluid which should be treated. As a result, a fourth layer called fluid layer is formed. The carrier materiel is needed in order to carry and to isolate the transducer from the fluid. The layer formed by the carrier material is often named carrier layer, but sometimes it is referred to as matching layer. Actually, when the carrier material provides some impedance matching functionality to transmit the sound energy into the structure, the carrier layer is called matching layer. The transducer is bonded to the carrier layer by adhesive material, which forms the fifth and so-called adhesive layer [3, 4]. Figure 2 depicts the layer structure of the resonator. Thus, there are five subsequent layers: transducer, adhesive, carrier or matching, fluid and reflector layers.

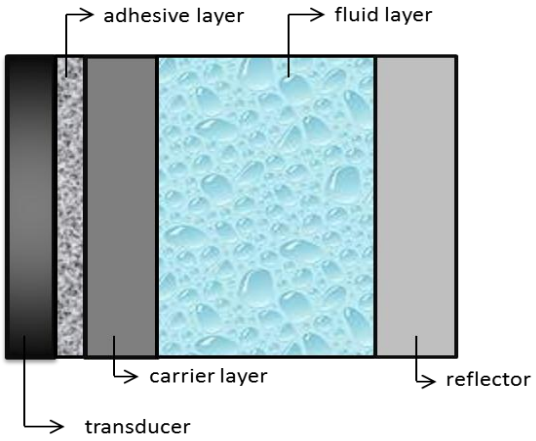

Figure 2 Structure of resonator, adapted from [5]

The most common way of generating ultrasound in fluids is by applying a piezoelectric transducer. This material converts electrical voltage into mechanical displacement [5].

2.3. Particles behaviour

The suspended particles, which are in the fluid layer of the resonator, experience forces when the suspension is in the ultrasonic field [3]. These forces influence particles behaviour as described below.

When the transducer is driven to excite a resonance frequency of the cavity, a standing wave with pressure minima and maxima occurs in the fluid layer. As a result, the particles are driven to the nodes within the field by axial primary radiation forces. Then, they are moved to the areas of maximum acoustic kinetic energy density within the plane by lateral force. These particular points are referred as acoustic “hot spots” by Schram [6]. Both forces – axial and lateral are caused due to the primary acoustic field. However, there is also a secondary radiation force. It is secondary acoustically generated force, which is produced from particle-particle interaction. The formation of

aggregates within the standing wave is assisted mainly by this force. Nevertheless, the contribution of the secondary radiation force is significant only when the particles are close enough to each other. If they are not in close proximity the force is negligible [5]. Figure 3 represents the behaviour of the particles within an ultrasonic field.

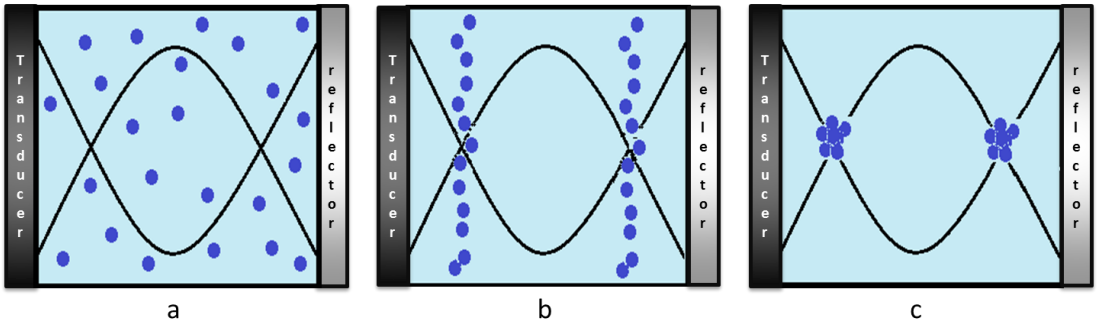

Figure 3 Behaviour of the particles within an ultrasonic field; (a) particles at the moment of turning on the transducer; (b) lines of particles at pressure nodal planes; (c) aggregation of the particles; adapted from [5]

2.4. Ultrasound enhanced sedimentation

The ultrasound enhanced sedimentation is the most common separation technique which was reported up to the late 1990s. It allows suspended particles to agglomerate under ultrasonic standing wave field due to the forces described in the section above. These agglomerates sediment when the ultrasonic field is nullified. The sedimentation is caused by the gravity force. Its importance increases over the viscous drag forces during the growth of agglomerates. Thus, the gravity force overcomes the viscous drag forces and sedimentation of the particles occurs [5]. Figure 4 represents the ultrasonic enhanced sedimentation in both case, when there is no aggregation of the particles (see figure 4a) and when there is aggregation of the particles (see figure 4b) during the time, when the ultrasonic field is switched on. The aggregation of particles depends on the particle-particle interaction.

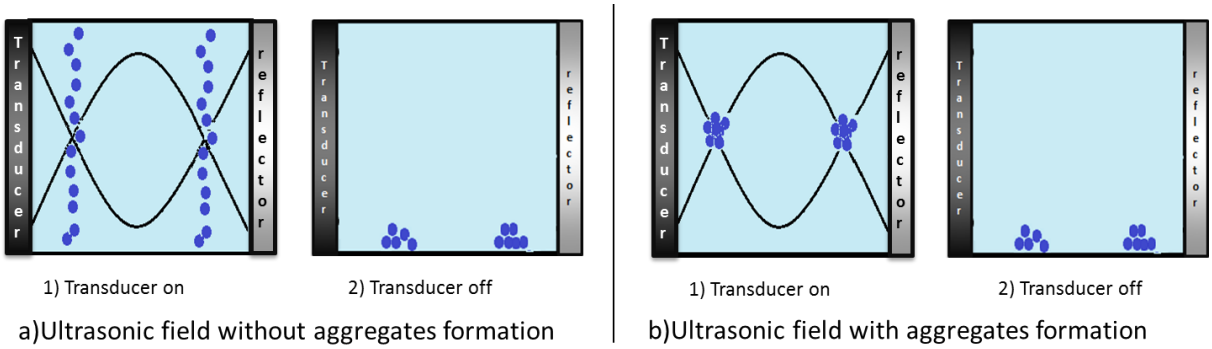

Figure 4 Ultrasound enhanced sedimentation

In summary, it can be said that the ultrasound enhanced sedimentation technique involves mainly two processes – 1) concentration of the particles and 2) their sedimentation. The suspended particles are concentrated due to the acoustic forces, which are results of the ultrasonic field. However, the sedimentation is based on gravity force. Therefore, the final separation is achieved due to the gravity force.
A device named BioSep employs the above discussed separation technique. It is used for separation of suspension in the current study.

2.5. Applications of ultrasonic field in solid-liquid separation

Many researchers have been recognized the high application potential of ultrasonic separation techniques especially in the field of biotechnology. The reported uses of ultrasonic standing wave field are mainly related to manipulation of biological cells [7]. The core reason is that the ultrasonic standing wave fields do not affect the cell viability. Consequently, the cells can be held and manipulated by the ultrasonic standing waves field without significant reduction in their viability [8-12]. For the first time Dyson [13] and Baker [14] described and reported the entrapment of blood cells in ultrasonic standing waves. Doblhoff-Dier et al. [9] and Wang et al. [11] performed experiments with mammalian cells. However, Gherardini et al. [15] did experiments with yeast cell. Bosma et al. [12] reported that ultrasound can be used for harvesting microalgae. It is reported by Cousins et al. that ultrasound can be used for preparation [16] and clarification [17] of plasma.

3. Materials and methods

In this chapter materials and methods, which were used during this study, are described. The chapter is divided into two main parts – *Modelling* and *Experiments*. The first part includes introduction to the BioSep's model, properties of the model and also a steady state analysis. Description of the experiments and their setups are included in the second part of the chapter.

The following materials were used: BioSep ADI 1015 (AppliSens), which consists of a control module (ADI 1015) and a resonator chamber (SonoSep ABF100.1); two peristaltic pumps with double-rotor pump head L/S EASY-LOAD MasterFlex 7518-00 (Cole-Parmer Instruments) ; off-line turbidity meter – MI 415 (Martini instruments); on-line turbidity meter, consisting of Turbidity Transmitter Trb 830 (Mettler-Toledo) and Data Acquisition System (DAQ); measurement chamber for the inline turbidity meter made of ABS; LabVIEW 2010 software (National Instruments); MATLAB R2011a software (MathWorks); magnetic stirrer RCT basic (IKA LaboRtechnic); scale LabStyle 303 (Mettler-Toledo); glass beakers; cylinders; 99% pure insoluble potato starch; clay; distilled water;

3.1. Modelling

The ultrasound enhanced sedimentation process, which occurs when BioSep is used for separation of suspensions, is modelled. The choices for system boundaries and variables are described. The chamber of Biosep is divided into three compartments, when the transducer is working (see figure 5). The first compartment includes the upper part of the Biosep's chamber, which starts from the beginning of the resonator. Thus, compartment 1 includes the volume bounded between the transducer and the reflector. However, it excludes the volume, which contains the suspended particles held by acoustic field and the liquid in their close proximity, which is actually the third compartment. The lower part of the BioSep's chamber is the second compartment. Every compartment is characterized by its own volume and concentration of suspended particles. The concentrations in the three compartments are chosen to be system variables.

The model is built up considering the following facts:

I) The Biosep has one inlet and two outlets – one for filtrate solution and one for concentrate solution. There are two pumps, which determine the filtrate flow rate (Q_1) and the concentrate flow rate (Q_2) respectively. At the current setting pump 1, which is related to the filtrate flow rate, is dependent on the transducer, but pump 2 is independent on it. When the transducer is working, pump 1 is also working. However, pump 1 stops working, when the transducer is switched off. In order to describe the work of the transducer, a transducer coefficient (α) is introduced. The transducer coefficient is chosen in this way that it can have only two values – 1 and 0. When transducer coefficient is 1, this means that transducer is switched on and the ultrasonic field is generated. On the other hand, when the transducer is switched off, the transducer coefficient is equal to 0.

II) The ultrasonic field is generated by the resonator and it plays the role of concentrator. Hence, a concentration reaction takes place between compartment 1 and compartment 3. This reaction is characterized by concentration coefficient (k_1), which is expected to have properties of rate constant.

III) When the transducer is switched off, the third compartment no longer exists due to the lack of ultrasonic field. Therefore, a reverse reaction of the concentration occurs. Suspended particles from compartment 3 are released to compartment 1. This reverse reaction also has its own coefficient, called reverse concentration coefficient (k_3). Similarly to the concentration coefficient, the reverse concentration coefficient should also have properties of rate constant.

IV) In addition to the reverse reaction, a settling reaction occurs. It is assumed that this reaction takes place between the first and the second compartments. It is characterized by settling coefficient (k_2). This coefficient is considered as a rate constant of settling reaction.

V) The losses from the first compartment to the second one due to turbulence flow during the ultrasonic field are also taken into account by introducing loss coefficient (k_4).

Figure 5 is a schematic representation of BioSep and its division into three compartments.

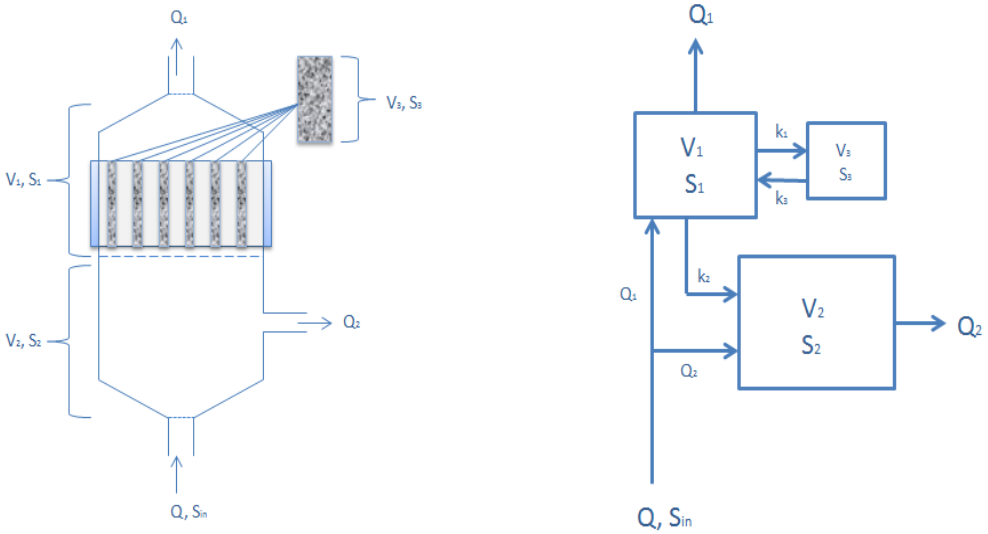

Figure 5 Schematic representation of BioSep

3.1.1. BioSep Model

The mass balances are set over each of the three compartments of the BioSep. As a result, the following model, which gives the relationship between the system variables, is obtained:

$$V_1 * \frac{dS_1}{dt} = Q_1 * S_{in} - Q_1 * S_1 + (1-\alpha) * k_3 * S_3 * V_3 - \alpha * k_1 * S_1 * V_1 - \frac{k_2 * S_1 * V_1}{Q_1 + k_4} \quad (1)$$

$$V_2 * \frac{dS_2}{dt} = Q_2 * S_{in} - Q_2 * S_2 + \frac{k_2 * S_1 * V_1}{Q_1 + k_4} \quad (2)$$

$$V_3 * \frac{dS_3}{dt} = \alpha * k_1 * S_1 * V_1 - (1-\alpha) * k_3 * S_3 * V_3 \quad (3)$$

Equation 1 represents the mass balance over the first compartment. The change of the total mass of suspended particles in compartment 1 over the time is due to 1) incoming particles from the sock solution ($Q_1 * S_{in}$); 2) outgoing particles from compartment 1 to filtrate solution ($Q_1 * S_1$); 3) outgoing particles from compartment 1 to compartment 3 because of the concentration reaction result from the ultrasonic field ($\alpha * k_1 * S_1 * V_1$); 4) incoming particles from compartment 3 during the reverse concentration reaction, when the ultrasonic field is nullified ($(1-\alpha) * k_3 * S_3 * V_3$) and 5) settling of particles from compartment 1 to compartment 2 $\left(\frac{k_2 * S_1 * V_1}{Q_1 + k_4}\right)$.

Equation 2 describes the change of the total mass of suspended particles in the second compartment over the time. The change is caused by 1) incoming particles from the sock solution ($Q_2 * S_{in}$); 2) outgoing particles from compartment 2 to concentrate solution ($Q_2 * S_2$); and 3) incoming particles from compartment 1 due to settling reaction $\left(\frac{k_2 * S_1 * V_1}{Q_1 + k_4}\right)$.

The change of the total mass of suspended particles in the third compartment over the time is defined by equation 3. The reasons for the change are: 1) incoming particles from compartment 1 due to the concentration reaction, which is a result of the ultrasonic field ($\alpha * k_1 * S_1 * V_1$); and 2) outgoing particles from compartment 3 to compartment 1 during the reverse concentration reaction, when the ultrasonic field is switched off ($(1-\alpha) * k_3 * S_3 * V_3$).

In general the state space form of BioSep's model is given by the state equation and the output equation:

$$\dot{S} = \begin{pmatrix} \frac{dS_1}{dt} \\ \frac{dS_2}{dt} \\ \frac{dS_3}{dt} \end{pmatrix} = \begin{pmatrix} \frac{Q_1 * S_{in}}{V_1} - \frac{Q_1 * S_1}{V_1} + \frac{(1-\alpha) * k_3 * S_3 * V_3}{V_1} - \alpha * k_1 * S_1 - \frac{k_2 * S_1}{Q_1 + k_4} \\ \frac{Q_2 * S_{in}}{V_2} - \frac{Q_2 * S_2}{V_2} + \frac{k_2 * S_1 * V_1}{V_2 * (Q_1 + k_4)} \\ \frac{\alpha * k_1 * S_1 * V_1}{V_3} - (1-\alpha) * k_3 * S_3 \end{pmatrix} \quad (4)$$

$$S = \begin{pmatrix} S_1 \\ S_2 \\ S_3 \end{pmatrix} \quad (5)$$

Where S_1, S_2 and S_3 are the states, Q_1, Q_2 and α are the control inputs and S_{in} is the disturbance input. In this case (see eq.5), the outputs are the concentration of suspended particles in the three compartments, which are actually the states of the systems.

Linearization around steady state of the BioSep's model is presented in Appendix I in state space form.

3.1.2. System properties

Properties of the BioSep are the main focus in this part. Special attention is paid to observability and controllability for on-line estimation and control.

Dynamics

BioSep is a dynamic system because it is described by set of differential equations (eq. 1-3). This system has a memory; its output at any time instant depends not only on the present input but also on its history.

Linearity

The differential equations 1-3 are non-linear as they contain products of the states and inputs. Consequently, the system described by these equations is a non-linear and it does not satisfy the superposition principle. Linearization of the system around steady state is presented in Appendix I.

Time-invariance

The system is time-invariant because the system equations do not vary in time. Hence, time does not appear explicitly neither in $f(x,u,p)$ nor in $g(x,u,p)$ (see Appendix I).

Causality

The considering system is a physical system. Consequently, the outputs of the system depend only on current and past inputs but they are independent of the future inputs. Thus, the BioSep is a causal system.

Observability and Controllability

Observability and controllability are important system properties for further development of observer and control strategies. In order to see what is going on inside the system using input-output measurements, the system must be observable. Moreover, in order to be able to do whatever it is wanted with the given dynamic system under control inputs, the system must be controllable. These two properties are examined for the linearized system around steady state by Matlab's symbolic toolbox, because as yet the parameters and the initial conditions in the model of the systems are unknown. For each property two cases are analysed – when the transducer is switched on and when it is switched off (see Appendix II). Because these two possible cases for the transducer coefficient, which is one of the inputs in the system, are studied, the number of the inputs decreases with one; from four to three. Matlab's script is presented in Appendix III.

Stability is other important property of the system. The system stability is determined by the real part of eigenvalues of the system. Consequently, this system property cannot be examined by the symbolic toolbox because the toolbox will give expressions for the eigenvalues but not exact numbers. Therefore, the stability is not included here. However, when the parameters are estimated the stability of the system can be easily studied. If the real part of all eigenvalues is less than zero, the system will be called asymptotically stable. If the real part of all eigenvalues is equal to zero or if just one of the eigenvalues has real part equal to zero and the rest are less than zero, the system will be stable. In all other cases, the system will be unstable.

Case I: when the transducer is switched on, transducer coefficient is equal to 1 ($\alpha = 1$)

When the transducer is switched on, the A, B and C matrices become the following ones:

$$A_1 = \begin{pmatrix} -\frac{Q_1}{V_1} - k_1 - \frac{k_2}{Q_1+k_4} & 0 & 0 \\ \frac{k_2*V_1}{V_2*(Q_1+k_4)} & -\frac{Q_2}{V_2} & 0 \\ \frac{k_1*V_1}{V_3} & 0 & 0 \end{pmatrix} (6);\ B_1 = \begin{pmatrix} \frac{S_{in}}{V_1} - \frac{S_1}{V_1} + \frac{k_2*S_1}{(Q_1+k_4)^2} & 0 & \frac{Q_1}{V_1} \\ -\frac{k_2*S_1*V_1}{V_2*(Q_1+k_4)^2} & \frac{S_{in}}{V_2} - \frac{S_2}{V_2} & \frac{Q_2}{V_2} \\ 0 & 0 & 0 \end{pmatrix} (7);\ C_1 = \begin{pmatrix} 1 & 0 & 0 \\ 0 & 1 & 0 \\ 0 & 0 & 1 \end{pmatrix} (8);$$

All variables are in steady state. The linearized state space form of the system is presented in Appendix II.

In order to examine the observability of the system, the observability matrix is defined as:

$$O_1 = \begin{pmatrix} C_1 \\ C_1A_1 \\ C_1A_1^2 \end{pmatrix} \quad (9)$$

According to the result from Matlab (see Appendix III for the script) the system in this case is observable due to full column rank of the observability matrix.

The controllability is also examined. The controllability matrix consisting of the A_1 and B_1 matrices is defined as:

$$R_1 = \begin{pmatrix} B_1 & A_1B_1 & A_1^2B_1 \end{pmatrix} \quad (10)$$

According to the result from Matlab (see Appendix III for the script) the controllability matrix has full column rank. Therefore, the system (A_1, B_1, C_1, D_1) is controllable.

O_1 and R_1 are not presented here as they contain too complex expressions.

Case II: when the transducer is switched off, transducer coefficient is equal to 0 ($\alpha = 0$)

Similarly, using the same methodology the observability and controllability are studied in the second case, when the transducer is switched off. In this case, the A, B and C matrices become the following:

$$A_2 = \begin{pmatrix} -\frac{Q_1}{V_1} - \frac{k_2}{Q_1+k_4} & 0 & \frac{k_3*V_3}{V_1} \\ \frac{k_2*V_1}{V_2*(Q_1+k_4)} & -\frac{Q_2}{V_2} & 0 \\ 0 & 0 & -k_3 \end{pmatrix} (11);\ B_2 = \begin{pmatrix} \frac{S_{in}}{V_1} - \frac{S_1}{V_1} + \frac{k_2*S_1}{(Q_1+k_4)^2} & 0 & \frac{Q_1}{V_1} \\ -\frac{k_2*S_1*V_1}{V_2*(Q_1+k_4)^2} & \frac{S_{in}}{V_2} - \frac{S_2}{V_2} & \frac{Q_2}{V_2} \\ 0 & 0 & 0 \end{pmatrix} (12);\ C_2 = \begin{pmatrix} 1 & 0 & 0 \\ 0 & 1 & 0 \\ 0 & 0 & 1 \end{pmatrix} (13);$$

All variables are in steady state. In Appendix II state space representation of the linearized system is presented. The C matrix is independent of the value of transducer coefficient. That is the reason why C_1 and C_2 are the same.

In this case the observability and controllability matrix are defined as:

$$O_2 = \begin{pmatrix} C_2 \\ C_2A_2 \\ C_2A_2^2 \end{pmatrix} \quad (14); \qquad R_2 = \begin{pmatrix} B_2 & A_2B_2 & A_2^2B_2 \end{pmatrix} \quad (15);$$

According to Matlab the system in this case is observable because of the full column rank of the observability matrix and uncontrollable due to the fact that controllability matrix does not have full row rank (see Appendix III for the script). O_2 and R_2 are not presented here as they contains too complex expressions.

3.1.3. Steady state analysis

Steady state analysis is performed in this chapter in order to see which parameters can be determined from the steady states.

If the system is at steady state, there is no change in the states with the time. Therefore, all derivatives with respect to time are zero. Thus, the equations 1-3, described above in this chapter (see section *3.1.1. Model*) become the following:

$$(1-\alpha)*k_3*S_{3ss}*V_3-\alpha*k_1*S_{1ss}*V_1-\frac{k_2*S_{1ss}*V_1}{Q_1+k_4}=Q_1*(S_{1ss}-S_{in}) \quad (16)$$

$$\frac{k_2*S_{1ss}*V_1}{Q_1+k_4}=Q_2*(S_{2ss}-S_{in}) \quad (17)$$

$$\alpha*k_1*S_{1ss}*V_1-(1-\alpha)*k_3*S_{3ss}*V_3=0 \quad (18)$$

Derivations of these equations are presented in Appendix IV.

It should be taken into account that steady state for the concentration in compartment 3 (S_3) is not always possible. When the transducer is switched on ($\alpha=1$), concentration reaction of suspended particles from compartment 1 to compartment 3 occurs. Therefore, constant increase of the concentration in compartment 3 is expected. The concentration will go to infinity if the concentration reaction is continuous. As a result, there is no steady state value that can be reached and thus, the equation 18 is not valid in this case.

When $\alpha=1$, equation 18 becomes:

$$k_1*S_{1sson}*V_1=0 \quad (19)$$

Most likely, equation 19 is mathematically not valid because all components in the left-hand side in it are expected to be different from zero. Consequently, it can be concluded that the equation 18 does not hold in the case when $\alpha=1$.

However, when the transducer is turned off ($\alpha=0$), the concentration reaction ends and the reverse reaction occurs. Thus, the concentration in compartment 3 eventually becomes zero ($S_3=0$). Therefore, it can be accepted that this is the steady state value for the concentration in compartment 3 in this case.

When $\alpha=0$, equation 18 becomes:

$$-k_3*S_{3ssoff}*V_3=0 \quad (20)$$

Equation 20 is valid only when at least one of its components in the left-hand side is equal to zero. Because the volume of compartment 3 is different from zero and k_3 is expected to be different from zero, the only case when the equation 20 holds is when S_{3ssoff} is zero.

Briefly, it can be said that the steady state for the concentration of suspended particles in compartment 3 (S_{3ss}) is possible only when the transducer is switched off ($\alpha = 0$).

Considering equations 16, 17 and 18 the following linear regression is derived:

$$\begin{pmatrix} -\alpha * S_{1ss} * V_1 & -S_{1ss} * V_1 & (1-\alpha) * S_{3ss} * V_3 \\ 0 & S_{1ss} * V_1 & 0 \\ \alpha * S_{1ss} * V_1 & 0 & -(1-\alpha) * S_{3ss} * V_3 \end{pmatrix} \begin{pmatrix} k_1 \\ k_2 \\ \hline Q_1 + k_4 \\ k_3 \end{pmatrix} = \begin{pmatrix} Q_1 * (S_{1ss} - S_{in}) \\ Q_2 * (S_{2ss} - S_{in}) \\ 0^1 \end{pmatrix} \quad (21)$$

Generally, there are four unknown parameters – k_1, k_2, k_3, k_4 and three equations. Because S_3 cannot be measured and thus it is unknown as well and because the product of k_3 and S_3 appears in all equations, the product can be assumed as unknown. Still the numbers of unknowns are more than the numbers of equations. However, simplification occurs if two cases for the transducer, when it is switched on ($\alpha = 1$) and when it is switched off ($\alpha = 0$), are analyzed separately (see Appendix IV).

Case I: when the transducer is switched on, transducer coefficient is equal to 1 ($\alpha = 1$)

The following expressions for k_1 and k_2 are found when the transducer is switched on from the linear regression:

$$\widehat{k_1} = -\frac{Q_1 * (S_{1sson} - S_{in}) + Q_2 * (S_{2sson} - S_{in})}{S_{1sson} * V_1} \quad (22)$$

$$\widehat{k_2} = \frac{Q_1 * Q_2 * (S_{2sson} - S_{in})}{S_{1sson} * V_1} \quad (23)$$

K_1 can also be expressed as:

$$\widehat{k_1} = -\frac{Q_1 * (S_{1sson} - S_{in})}{S_{1sson} * V_1} - \frac{\widehat{k_2}}{Q_1} \quad (24)$$

Explicit derivation of these equations can be seen in Appendix IV.

Case II: when the transducer is off, transducer coefficient is equal to 0 ($\alpha = 0$)

The following expression for k_4 is obtained when the transducer is switched off:

$$\widehat{k_4} = \frac{S_{1ssoff} * V_1 * \widehat{k_2}}{Q_2 * (S_{2ssoff} - S_{in})} \quad (25)$$

In this case it is taking into account that when the transducer coefficient is equal to zero ($\alpha = 0$), the filtrate flow rate is also equal to zero ($Q_1 = 0$). Explicit derivation of this equation is presented in Appendix IV.

[1] The third row of the linear regression (21) is valid only when the transducer is switched off ($\alpha = 0$) because only then then S_3 has steady state value.

Although a steady state for the concentration of suspended particles in compartment 3 exists in this case, it cannot be use for estimation of k_3.

In summary, from this analysis is clear that only three out of four parameters can be determine from the steady states, namely k_1, k_2 and k_4 . The first two parameters ($k_1$and k_2) are derived from the first case, when the transducer is switched on. However, k_4, the third parameter is derived from the second case, when the transducer is switched off. As a result, only one parameter, k_3, is still unknown. However, it can be estimate from the dynamic data (see section *4.2.4. Estimation of* k_3).

3.2. Experiments

In this part all of the experiments performed during this study are described. Mainly, there are two sets of experiments. The first one is related to determination of the ratio between filtrate and concentrate flow rate in order to obtain the highest separation efficiency, thus the best separation. The second one is the dynamic experiments.

3.2.2. Determination of the ratio between filtrate and concentrate flow rate for the best separation

In order to determine the ratio between filtrate and concentrate flow rate for the best separation the experimental setup shown in figure 6 was used.

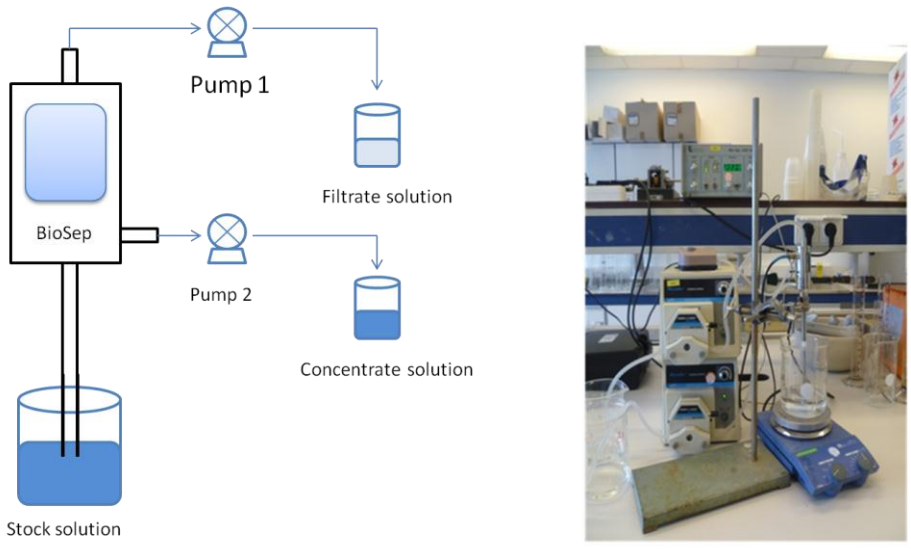

a) Schematic representation **b) Experimental setup**

Figure 6 Experimental setup for the first set of experiments

The BioSep chamber was connected to both pumps - pump 1, which determined the filtrate flow rate and pump 2, which determined the concentrate flow rate. Solutions of clay with three different concentrations – 3.33 g/L, 1.67 g/L and 0.83 g/L were prepared. These clay solutions were used as stock solutions. The BioSep was submerged in the stock solution. Then, both pumps were switched on and BioSep chamber was filled up with it. After that the pumps were switched off. Adjustment of the resonance frequency of the field to the desired value of 2.1 MHz was done. Moreover, the time for on- and off-period of the ultrasonic field was set by a timer on the ADI 1015. A cycle consisting of

3 seconds off-period, when the ultrasonic field was switched off and 30 seconds on-period, when the ultrasonic field was switched on, was chosen. Pump 1 was connected to the ADI 1015 controller. As a result, the pump was working when the ultrasonic field was switched on. However, pump 2 was not connected to the controller; thus, it was working during the whole cycle – on and off-period. The rate of both pumps, which resulted in different flow rates, differed in every experiment. The whole range of pump rates (from 1 to 10), hence, the whole range of flow rates, were covered for every concentration of the stock solution by adjusting the knobs for the pump rates. After all settings were made, the ultrasonic field and the timer were switched on and separation process started. During one experiment ten cycles of 33 seconds were running. The stock solution was continuously stirred by magnetic stirrer. Filtrate and concentrate solutions were collected separately. Then their volumes and turbidity were measured. Every turbidity measurement was repeated three times and the average value was used for further data analysis. In this set of experiments the off-line turbidity meter was used.

3.2.3. Dynamic experiments

In order to have dynamic measurements of the suspended particles concentration in the filtrate and concentrate solution as well as in the stock solution, when the optimal pump ratio between concentrate and filtrate flow rates was used, an in-line turbidity meter was installed in the setup. The in-line turbidity meter was put in a measurement chamber made of ABS material, which is referred as turbidity measurement chamber in figure 7, 8 and 9. The turbidity meter was connected to DAQ system and computer. A time step of the measurements was fixed to 0.2 second. In this set of experiments, 0.83 g/L starch solution was used as stock solution. The experiments were repeated three times. For each repetition new stock solution with 0.83 g/L was prepared. There were three different setups depending on which concentration was measured, as described below.

3.2.3.1. Dynamic measurements of concentration in the stock solution

The dynamic measurements of the concentration of suspended particles in the stock solution were obtained by using the setup depicted in figure 7.

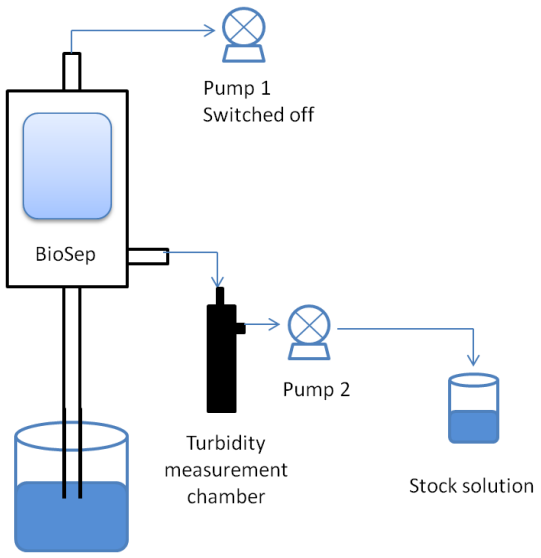

Figure 7 Schematic representation of the experimental setup for dynamic measurements of the suspended particles concentration in the stock solution

The BioSep chamber was connected to both pumps. The ABS measurement chamber with the in-line turbidity meter (turbidity measurement chamber in figure 7) was connected to the outlet of the BioSep, which in turn was connected to pump 2. The BioSep was submerged in the stock solution. Then, both pumps were switched on and BioSep chamber was filled up with it. After that the pumps were switched off. In this case the ultrasonic field was not switched on during the whole experiment; thus, no adjustments of the resonance frequency and of the on- and off-period were needed. Moreover, only pump 2 was used; so only its pump rate was adjusted to 6.8 (the knob's position for the rate of pump 2 is 6.8). This value of the rate of pump 2 simulated the average incoming flow rate of stock solution during one cycle, when the optimal ratio between the rates of the two pumps was used (see Appendix V). The stock solution was continuously stirred by magnetic stirrer. Measurements collection started when the pump 2 was switched on. The turbidity of the stock solution was also measured with off-line turbidity meter, three times.

3.2.3.2. Dynamic measurements of concentration in the filtrate solution

The dynamic measurements of the concentration of suspended particles in the filtrate solution were obtained using the setup shown in figure 8.

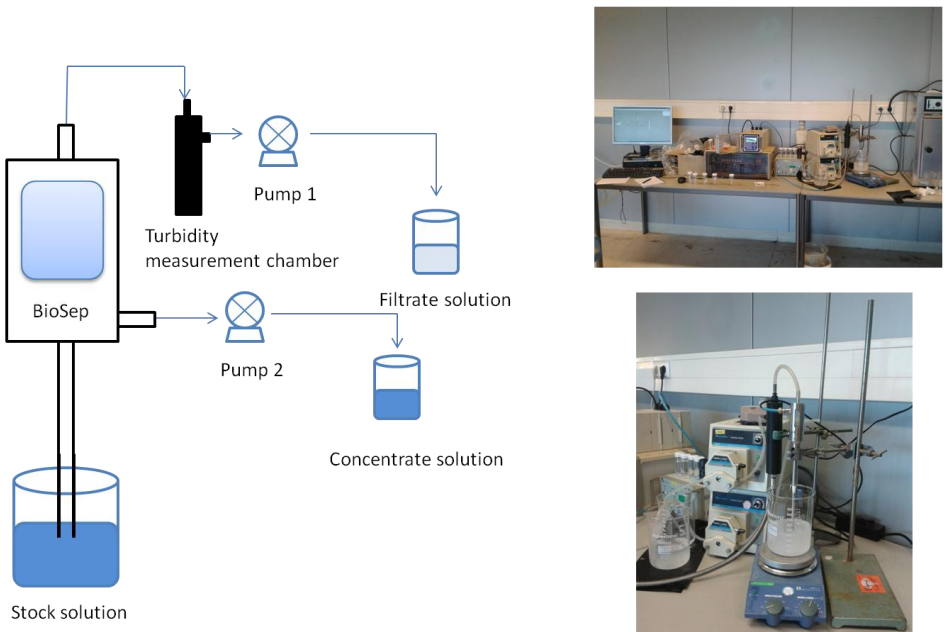

a) Schematic representation **b) Experimental setup**

Figure 8 Experimental setup for dynamic measurements of the suspended particles concentration in the filtrate solution

The BioSep chamber was connected to both pumps. The turbidity measurement chamber was installed between the BioSep and the pump 1. The BioSep was submerged in the stock solution. Then, both pumps were switched on and the BioSep chamber was filled up with the stock solution. After that the pumps were switched off. Adjustment of the resonance frequency of the field (2.1MHz), of the cycle time (3s off-period and 30s on-period) and of the rate of both pumps (rate of pump 1– 2 and rate of pump 2 - 5, which was the optimal ratio) were done. Pump 1 was connected

to the ADI 1015 controller. As a result, the pump was working only during the on-period, when the ultrasonic field was switched on. However, pump 2 was not connected to the controller; thus, it was working during the whole cycle – during the both periods (on- and off-period). After all settings were made, the ultrasonic field and the timer were switched on and the separation process and the measurement collection of the concentration of suspended particles in the filtrate solution started. The stock solution was continuously stirred by magnetic stirrer. Filtrate and concentrate solutions were collected separately. The turbidity of the stock, filtrate and concentrate solution was also measured with off-line turbidity meter. Each turbidity measurement was repeated three times.

3.2.3.3. Dynamic measurements of concentration in concentrate solution

The concentration of suspended particles in the concentrate solution over the time during the separation process was obtained by using the setup depicted in figure 9. It is similar to the setup used for dynamic measurements of the concentration of suspended particles in the filtrate solution, but in this case the in-line turbidity meter was connected to pump 2, not to pump 1 as in the previous case (see figure 8).

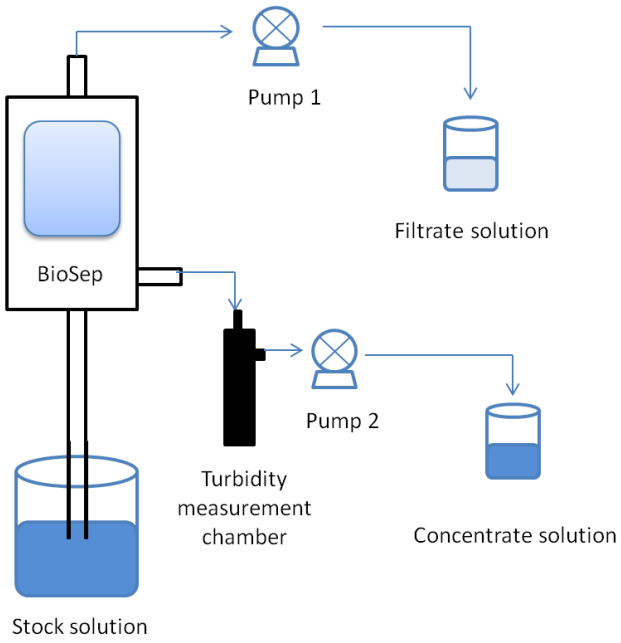

Figure 9 Schematic representation of the experimental set-up for dynamic measurements of the suspended particles concentration in the concentrate solution

The BoSep chamber was connected to both pumps. The ABS measurement chamber with the in-line turbidity meter (turbidity measurement chamber in figure 9) was installed between the BioSep and the pump 2. The BioSep was submerged in the stock solution. Then, both pumps were switched on and BioSep chamber was filled up. After that the pumps were switched off. Adjustment of the resonance frequency of the field (2.1MHz), of the cycle time (3s off-period and 30s on-period) and of the rate of both pumps (rate of pump 1 – 2 and rate of pump 2 - 5, which was the optimal ratio) were done. Pump 1 was connected to the ADI 1015 controller, but pump 2 was not. As a result, the pump 1 was working only when the ultrasonic field was switched on. In contrast, pump 2 was working during the whole cycle, during the both periods when the ultrasonic field was switched on and off.

After all settings were made, the ultrasonic field and the timer were switched on and the separation process and the measurement collection of the concentration of suspended particles in the concentrate solution started. The stock solution was continuously stirred by magnetic stirrer. Filtrate and concentrate solutions were collected separately. The turbidity of the stock, filtrate and concentrate solution was also measured with off-line turbidity meter. Each turbidity measurement was repeated three times.

4. Results and Discussion

In this chapter the results from the experiments are shown and discussed. The chapter is divided into three main parts – experiments, parameter estimation and control strategy.

4.1. Experiments

4.1.1. Determination of the ratio between filtrate and concentrate flow rate for the best separation

The volume and the turbidity of both solutions – filtrate and concentrate at different flow rates were obtained from the first set of experiments as was described in the experimental part of *Materials and Methods* (see *3.2.1 Determination of the ratio between filtrate and concentrate flow rate for the best separation*). For each combination of the rates of both pumps for certain concentration of clay solution, filtrate and concentrate flow rates were calculated taking into account the measured volumes of the filtrate and concentrate solution respectively and the working time of the pumps during the experiments. Due to the fact, that pump 1 was connected to the ADI 1015 controller and hence, it was working only during on-periods of the ten cycles, its working time was 300 seconds. However, the working time of pump 2 was equal to the time for one whole experiment because it was working during both periods on- and off-. Thus, the working time of pump 2 was 330 seconds. Moreover, separation efficiency is also calculated. It was defined as difference between turbidity of the concentrate and filtrate solution. Then the rates of both pumps and the separation efficiency for certain concentration were plotted in a 3D-mesh plot. It can be seen from figure 10 that the best separation, when clay solution with 3.33 g/L concentration was used, was obtained when the rate of pump 1 and 2 were 2 and 5 respectively. Table 1 represents in summary the results from this set of experiments. It shows the rates of both pumps, at which the highest separation efficiency was obtained for each clay suspension.

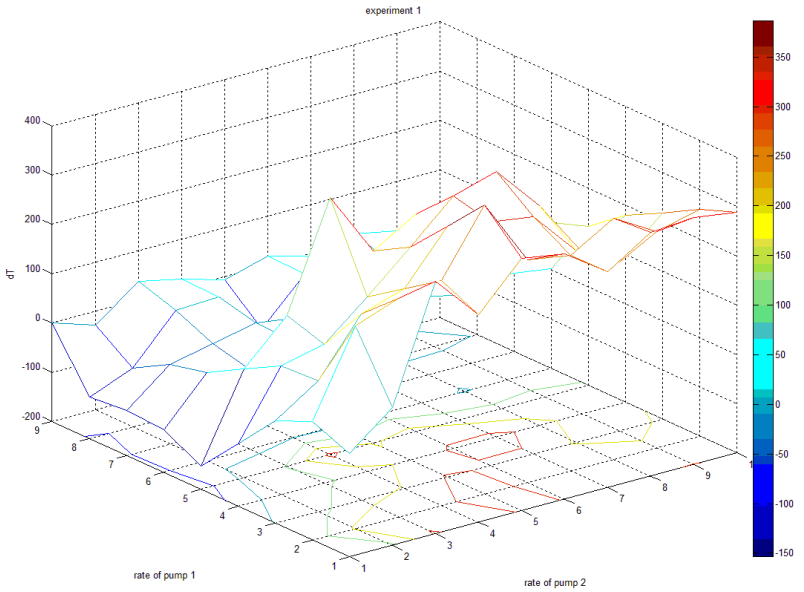

Figure 10 3D-mesh plot for experiment 1 – 3.33 g/L clay solution

Table 1 Rates of both pumps for best separation

Experiment	C [g/L]	Rate of pump 1	Rate of pump 2
1	3.33	2	5
2	1.67	3	5
3	0.83	2	6
average	-	2.3	5.3

The average values for the rates of pump 1 and 2 are 2.3 and 5.3 respectively. However, since the knobs for the pump rate cannot be adjusted so accurate in practice, the value of 2 for pump 1 and value of 5 for pump 2 are chosen for further experiments. These pump rates determine filtrate flow rate of 0.46 ml/s and concentrate flow rate of 1.38 ml/s.

4.1.2. Dynamic experiments

Dynamic measurements of the suspended particles concentration in filtrate, concentrate and stock solution were obtained from the second set of experiments as was described in the experimental part of *Materials and Methods* (see *3.2.2 Dynamic experiments*). Correction of the off-set of these dynamic measurements was done by off-line turbidity meter on the average basis. Because the on-line turbidity meter measured directly the concentration of the particles and the off-line one measured only the turbidity of the solutions, a calibration curve was made using starch solutions with five different concentrations (0 g/L, 0.64 g/L, 1.26 g/L, 2.52 g/L, 5.00 g/L). After the correction all three measurements – concentration of suspended particles in the stock solution (S_{in}), filtrate solution (S_1) and concentrate solution (S_2) were combined and ploted. It is assumed that the compartment 1 and 2 are ideally mixed and thus, the concentration of suspended particles in the filtrate solution is the same as in compartment 1 and the concentration of suspended particles in the concentrate solution is the same as in compartment 2. As was described in the dynamic experiments section in *Materials and Methods* (see *3.2.2 Dynamic experiments*), three solutions with the same concentration of starch (0.83 g/L) were prepared and measured. Therefore, three graphs, one for each of these solutions were obtained (see Appendix VI). However, for further analysis and calculation the average data are considered.

Figure 11 represents the changes in the concentrations of interest $(S_{in}, S_1$ and $S_2)$ over the time using average data. It is obvious that separation occurs. There is a significant difference between the concentration in compartment 1 (green line in figure 11) and the concentration in compartment 2 (red line in figure 11). The expected significant difference between the concentrations in filtrate and in concentrate solution because of the assumption that compartment 1 and 2 are ideally mixed is also observed (see figure 12).

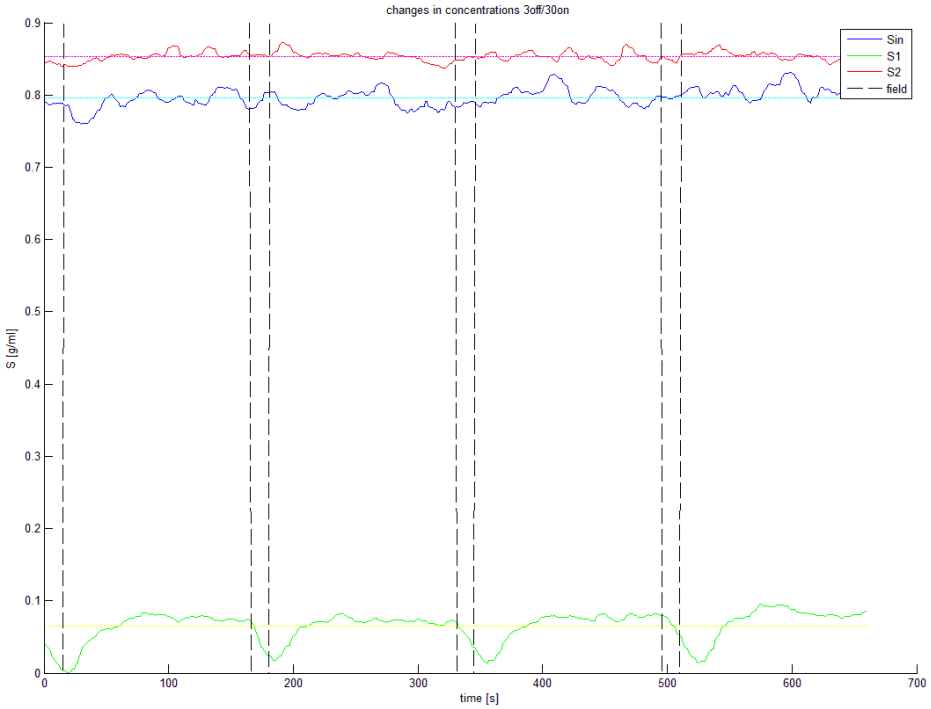

Figure 11 Dynamics of S_{in}, S_1 and S_2 of 0.83 g/L starch solution using average data

It can be seen from figure 11 that the concentration in the stock solution (S_{in}) as well as the concentration in compartment 2 (S_2) can be assumed as constant if the measurement noise is neglected. S_{in} was constant, therefore it was expected no changes in it over the time to occur. This expectation was confirmed by the dynamic measurements of S_{in}. However, it was unexpected S_2 to be constant over the time. Increase of S_2 during the off-periods, which resulted in peaks during these periods, was expected due to the settling reaction of particles from compartment 1 to compartment 2. Probably, because of the smaller volume of compartment 1 compared to compartment 2 and the same amount of total mass of particles, which were coming from the first to the second compartment, the additional effect of these incoming particles to the concentration in compartment 2 is small and it cannot be detected with this in-line turbidity meter. In other words, most likely this sensor is not so sensitive; therefore, the additional effect of the incoming particles from compartment 1 to compartment 2 cannot be distinguished from the noise.

Figure 11 also shows the changes of the concentration in compartment 1 (S_1) over the time. Expected drops in this concentration during the off-period due to the settling reaction of particles from compartment 1 to compartment 2 as well as expected increase of the concentration in compartment 1 at the beginning of the on-period due to new portions of incoming stock solution can be seen in figure 11. It can also be seen that S_1 reaches its steady state values during the on-period (S_{1sson}). This was also expected because the inflow of new portions stock solution and the outflow of the filtrate solution as well as concentration reaction of particles from compartment 1 to compartment 3 were fixed, so they had constant values. However, at the beginning of the off-period first an increase of S_1 was expected due to reverse concentration reaction, which released particles from compartment 3 to compartment 1, and then, a decrease in S_1 was expected during the off-

period because of the settling reaction of particles from compartment 1 to compartment 2. As mentioned above only the decrease is observed, but not the expected increase in the beginning of the off-period. Most likely, this is because of the small additional effect of the particles, released from compartment 3 to compartment 1, to the S_1 concentration due to the big difference between the volumes of these compartments. Thus, because of the low sensitivity of the in-line turbidity meter this additional effect cannot be detected.

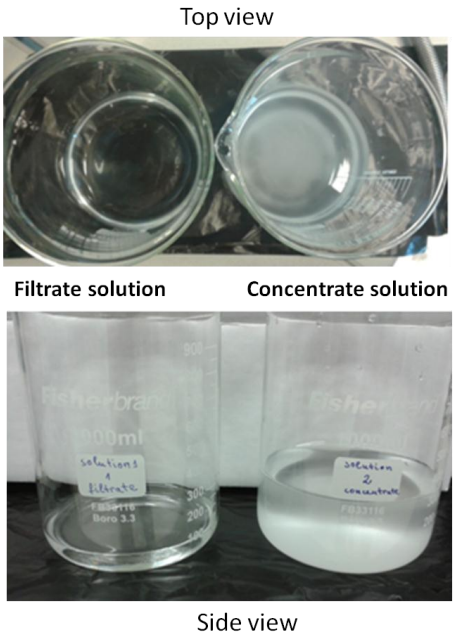

Figure 12 Filtrate and concentrate solution after separation of 0.83 g/L starch solution

4.2. Parameter Estimation

For parameter estimation the equations obtained from the steady state analysis and the data from the dynamic experiments were used. Three parameters can be determined from the steady state, namely k_1, k_2 and k_4 (see section *3.1.3 Steady state analysis*). However, in order to estimate these parameters, the steady state values of the states are needed as well as the volumes of the three compartments, the concentration of suspended particles in the stock solution and filtrate and concentrate flow rates.

With a known total volume (24 ml) and resonator volume (7 ml) of the BioSep and assuming that the volume of compartment 3 is 10% of the volume of compartment 1, the volumes of the three compartments were calculated. It was found that the volume of compartment 1 is 6.63 ml, the volume of compartment 2 is 17 ml and the volume of compartment 3 is 0.64 ml.

The rates of both pumps were fixed to 2 for pump 1 and to 5 for pump 2. These values determined respectively filtrate flow rate of 0.46 ml/s and concentrate flow rate of 1.38 ml/s.

The concentration of suspended particles in the stock solution (S_{in}) was calculated as average of all S_{in} measurements over the time. The outcome of this calculation is 0.797 g/L (see figure 11 – dark blue line – measured S_{in} ; light blue line –averaged S_{in}).

Steady state values of concentration of suspended particles in compartment 2 (S_{2ss}) and in compartment 1 (S_{1ss}) were calculated from the results of the dynamics experiments of starch solution.

The steady state value of S_{2ss} was calculated as average of all S_2 measurements over the time. It was found to be 0.853 g/L (see figure 11 – red line – measured S_2; pink line – steady state value of S_{2ss}). In order this calculation to be valid the following assumptions were made: 1) S_2 is at steady state all the time; 2) there is no difference between the steady state value of S_2, when the transducer is switched on (S_{2sson}) and its value, when the transducer is switched off (S_{2ssoff}) because S_2 is independent of the transducer (see eq. 17 in section *3.1.3 Steady state analysis*).

Because S_1 is dependent whether the transducer is working or not (see eq. 16 in section *3.1.3 Steady state analysis*), two cases are distinguished. Every case has its own steady state. Therefore, two values for steady state of S_1 are expected – when the transducer is switched on (S_{1sson}) and when the transducer is switched off (S_{1ssoff}). As can be seen from figure 11, S_1 reaches steady state during the on-period. From every cycle only the last sixty points of the on-periods were taken for the calculation of S_1. They were averaged and S_{1sson} of 0.075g/l was calculated. The steady state of S_1 was not observed during the off-periods (see figure 11). It was assumed that the last value of the line after the decrease of S_1 and before its increase again, in other words the minimum, was the steady state value of S_1 during the off-period (S_{1ssoff}). Similarly to the calculation of S_{1sson} , S_{1ssoff} was calculated by finding the average value of all three minima (the first minimum was excluded). As a result, 0.015g/l was calculated for S_{1ssoff}.

4.2.1. Estimation of k_2

Estimate of k_2 was calculated using equation 23 obtained from the first case of the steady state analysis, when the transducer is switched on (see eq. 23 in section *3.1.3 Steady state analysis, Case I*). $\widehat{K_2}$ was calculated to be 0.075 ml/s^2 after substitution.

4.2.2. Estimation of k_1

Estimate of k_1 was found using equation 24 obtained from the first case of the steady state analysis, when the transducer is switched on (see eq. 24 in section *3.1.3 Steady state analysis, Case I*). The calculated value for $\widehat{k_1}$ is 0.534 s^{-1}.

4.2.3. Estimation of k_4

Equation 25 for estimation of k_4 was obtained from the second case of the steady state analysis, when the transducer is switched off (see eq. 25 in *section 3.1.3 Steady state analysis, Case II*). $\widehat{k_4}$ was found to be 0.093 ml/s. This value is compared to the value of filtrate flow rate (Q_1) in order to check the assumption made in the first case of the steady state analysis, that filtrate flow rate is much higher than the loss coefficient. According to the values of k_4 (0.093 ml/s) and Q_1 (0.46 ml/s), the assumption is correct.

4.2.4. Estimation of k_3

The coefficient k_3 cannot be estimated from the steady state analysis. Dynamic data are needed. According to the BioSep model k_3 can be found from equation 1 or equation 3 only when the transducer is switched off ($\alpha = 0$) (see eq.1 and 3 in section *3.1.1 Model*).

When the transducer is off ($\alpha = 0$) , equation 1 becomes:

$$V_1 * \frac{dS_1}{dt} = Q_1 * S_{in} - Q_1 * S_1(t) + k_3 * S_3(t) * V_3 - \frac{k_2 * S_1(t) * V_1}{Q_1 + k_4} \quad (26)$$

When the transducer is off ($\alpha = 0$) , equation 3 becomes:

$$\frac{dS_3}{dt} = -k_3 * S_3(t) \quad (27)$$

Because there are only dynamic measurements of S_1 but not of S_3 from the dynamic experiments only the equation 26 is considered for further analysis.

Since the product of k_3 and $S_3(t)$ appears in equation 27, estimation of this product is done. After rearranging the equation, the following expression for the product $(k_3 * S_3(t))$ is achieved:

$$k_3 * S_3(t) = \frac{1}{V_3} * \left[V_1 * \frac{dS_1}{dt} - Q_1 * S_{in} + Q_1 * S_1(t) + \frac{k_2 * S_1(t) * V_1}{Q_1 + k_4}\right] \quad (28)$$

Thus, knowing $k_3 * S_3(t)$ and estimating the $S_3(t)$ from the mass conservation low, k_3 can be calculated. First, $S_3(t)$should be calculated using the following equation:

$$S_3(t) = \frac{1}{V_3} * [V_t * S_{in} - V_1 * S_1(t) - V_2 * S_2(t)] \quad (29)$$

Then, k_3 can be estimated from the following equation:

$$\widehat{k_3} = \frac{(k_3 * S_3(t))}{S_3(t)} = \frac{\left[V_1 * \frac{dS_1}{dt} - Q_1 * S_{in} + Q_1 * S_1(t) + \frac{k_2 * S_1(t) * V_1}{Q_1 + k_4}\right]}{[V_t * S_{in} - V_1 * S_1(t) - V_2 * S_2(t)]} \quad (30)$$

The derivative of S_1 with respect to time was calculated from the slope of the S_1 line obtained from the experiments during the off-periods. Due to the fact that there were three cycles, three slopes were calculated. The slopes in all three cycles were the same and they were equal to $-1*10^{-5}$. The graphs from which the slopes were obtained are presented in Appendix VII.

Only the first point of the off-period was taken for the estimation of k_3. The results from estimations of k_3 are shown in table 2. It is obvious that the value of k_3 from the second cycle is much different than the other two values. Thus, this value is excluded from the calculation of the average estimate of k_3. The averaged value of $\hat{k}_3$ was calculated to be 0.015 s^{-1}.

Table 2 Estimates of $\widehat{k}_3$ and $\widehat{S}_3$

cycle	$\widehat{k}_3$ [s^{-1}]	$\widehat{S}_3$ [g/ml]
1	0.011	0.0065
2	-0.002	0.0066
3	0.019	0.0065

4.2.5. Simulation with estimated parameters

Given the estimated values of the parameters, the output behaviour of the considering system which was linearized, is simulated by Matlab over period of one (33 s) and ten cycles (330 s) with time step of 0.1 seconds. The outputs of the systems are the three states – the concentrations of suspended particles in the three compartments (see Appendix VIII for the Matlab script). Figure 13 and 14 shows the dynamics of the system during one and ten cycles, respectively.

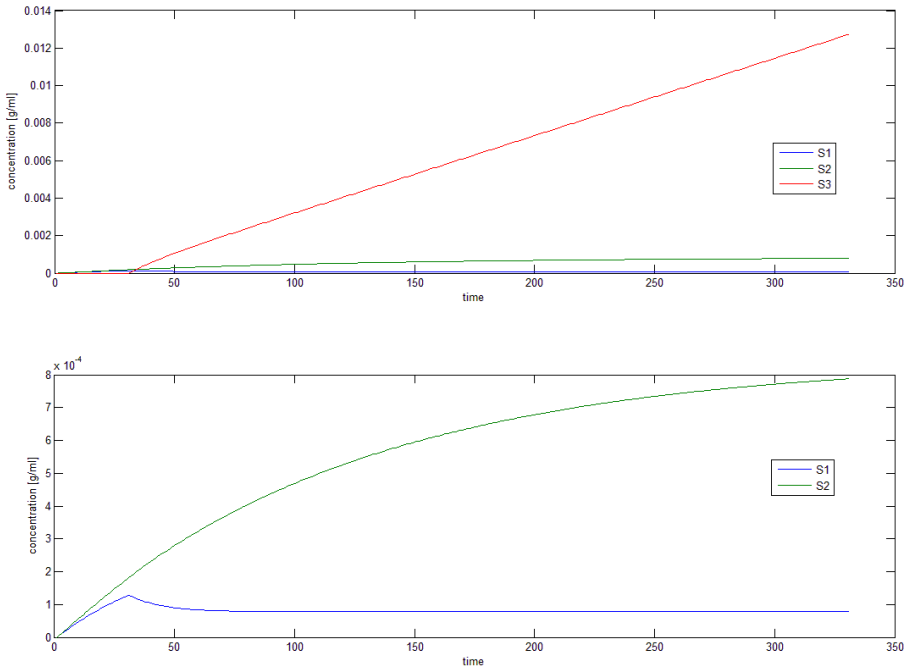

Figure 13 Simulation of the system behaviour over 1 cycle

The behaviour of the system, which is simulated over one cycle, is as it was expected. The cycle starts with off-period during which the concentrations of suspended particles in compartment 1 (blue line in figure 13) and in compartment 2 (green line in figure 13) increase due to the incoming stock solution. Because the ultrasonic field is not switched on, compartment 3 is not defined yet. Thus, the concentration in compartment 3 (red line in figure 13) is equal to zero during the off-period of the first cycle.

However, during the on-period the transducer is working and the ultrasonic field is generated. As a result, concentration reaction of particles from compartment 1 to compartment 3 takes place. Therefore, increase in concentration in compartment 3 and decrease in concentration in

compartment 1 can be seen in figure 13. After the decrease, the concentration in compartment 1 reaches constant value because the flow rate of incoming liquid to compartment 1 and the flow rate of outgoing liquid from it are fixed. Moreover, the concentration reaction that occurs during the on-period has constant rate due to the fixed ultrasonic field. On the other hand, the concentration in compartment 3 continues to increase during the on-period because of new portions of stock solution, which are coming to compartment 1 and because of the concentration reaction, which continuous to occur during the whole on-period. Consequently, the new portions of particles which are coming to compartment 1 are moved continuously during the whole on-period to compartment 3 due to the acoustic forces and thus the constant increase of the concentration in compartment 3 is observed (see figure 13). Moreover, the concentration in compartment 2 also increases during the on-period due to the constant income of new portion of stock solution to compartment 2 during the whole cycle.

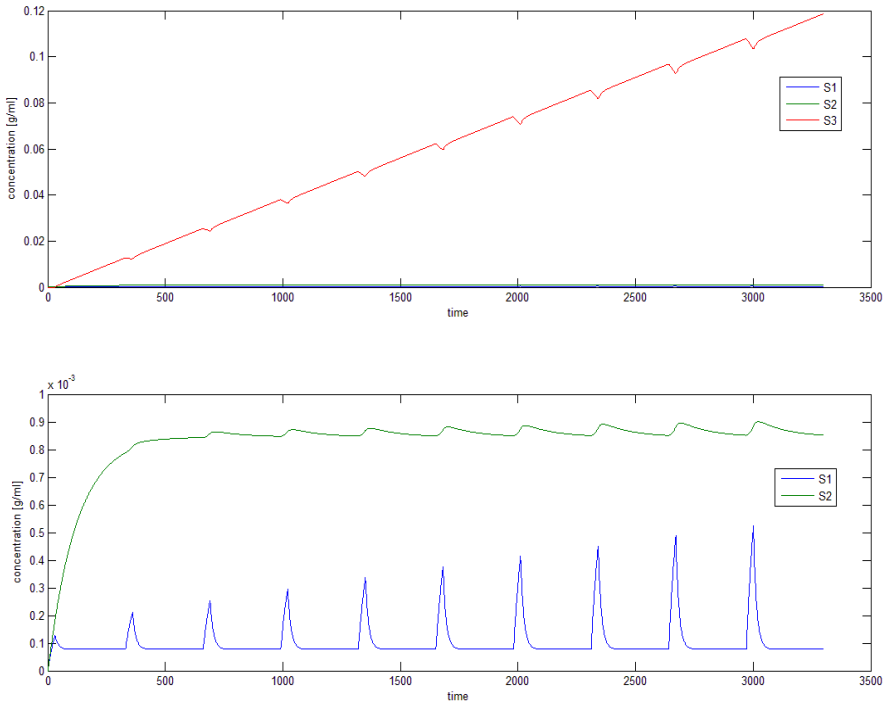

Figure 14 Simulation of the system behaviour over 10 cycles

Expected changes during the off- and on- period in all of the three concentrations as well as the overall change occurring after ten cycles can be seen in figure 14.

As it was expected during the off-periods, the concentration in compartment 1 (blue line in figure 14) first increases and then decreases. The increase is due to the fact that reverse concentration reaction takes place. The particles, collected by means of ultrasonic field in compartment 3 during the on-period, are released now from compartment 3 to compartment 1. However, during the off-period in addition to the reverse concentration reaction, a settling reaction also occurs. Due to this reaction

particles from compartment 1 settle to compartment 2. As a result, decrease in concentration in compartment 3 is observed.

From figure 14 it can also be seen that during the on-period S_1 reaches steady state value. It was also expected due to the fixed flow rates of incoming and outgoing liquid from this compartment and the constant rate of the concentration reaction of particles from compartment 1 to compartment 3.

The behaviour of the concentration in compartment 3 shown as red line in figure 14 was expected, too. The concentration in compartment 3 increases during the on-period because of the concentration reaction of particles from compartment 1 to compartment 3 and because of the continuous income of new portions of stock solution during this period. However, it decreases due to the reverse concentration reaction during the off-period. It is obvious that the this reaction is slower than the concentration reaction and the time for releasing the particles from compartment 3 to compartment 1 is not enough for all the particles to go to compartment 1.

Moreover, figure 14 shows that the concentration in compartment 2 increases during the off-period. The settling reaction of particles from compartment 1 to compartment 2 is the reason for that.

Because of the volume difference between the three compartment the length of the peaks and drops during the off-periods are different even though that the total mass of particles, which are transferred from one to the other compartment is the same. There are increase in the peaks and in the drops with the time because more particles are collected in compartment 3 with the time, more particles are released from it to compartment 1 and more particles are settled down from compartment 1 to compartment 2.

Generally, it can be said that the concentration in compartment 1 reach its steady state value every cycle during the on-period. Similarly, concentration in compartment 2 reaches its steady state value after the second cycle, again during its on-period (see figure 14). However, concentration in compartment 3 increases during the whole cycles except during the off-periods. All of these results were expected as it is discussed above. The only exception is the slow reverse concentration reaction, which results in slow release of particles from compartment 3 to compartment 1. It was expected this reaction to be faster and all the particles from compartment 3 to go to compartment 1 during the off-period. Thus, it was expected the concentration in compartment 3 during the off-periods to reach zero. The reverse reaction is described by the reverse concentration reaction coefficient (k_3). Therefore, the unexpected result indicates that probably k_3 was not estimated correctly and better parameter estimation has to be considered.

4.3. Control

In this section a design for open-loop control strategy is described. Switching control is considered. First, the optimal control strategy is selected and then behaviour of the controlled system is simulated.

4.3.1. Selection of the optimal control strategy

The general control problem focuses on finding control variables such that the controlled system behaves as it is desired. Therefore, first the desired behaviour of the system should be defined. In the current study, the highest possible separation efficiency in terms of difference in the total mass of

suspended particles between concentrate and filtrate solution after one cycle of 33 second is desired. Moreover, production of as pure as possible water is also wanted. The total mass of suspended particles in the filtrate solution determines the purity of the water. In addition to these objectives, there is another one – the separation process should be energy efficiency.

There are three control inputs – transducer coefficient (α), filtrate flow rate (Q_1) and concentrate flow rate (Q_2). Due to the fact that switching control is considered all of these inputs can have only two values. The transducer coefficient describes the working of the transducer and it can be either 1, when the transducer is switched on, or either 0, when the transducer is switched off. However, the filtrate and concentrate flow rate are determined by both pumps. When the pumps are working, their rates are fixed to the optimal pump rates, thus, the filtrate and concentrate flow rates are fixed to the optimal values, too. So when the pump 1 is switched off, Q_1 is 0 ml/s. However, when it is switched on, Q_1 is 0.46 ml/s. Similarly, when the pump 2 is switched off, Q_2 is 0 ml/s and when it is switched on, Q_2 is 1.38 ml/s (see section *4.1.1 Determination of the ratio between filtrate and concentrate flow rate for the best separation*). Eight possible combinations (2^3) of the three control inputs, which are considered, exist because each of the input can have only two values. Moreover, one cycle consists of two periods: a short one of 3 seconds and a long one of 30 seconds. Thus, there are eight combinations of the control inputs for each period during the cycle. As a result, there are sixty four (8*8) combinations of the control inputs, which represent 64 different control strategies. These different combinations of control inputs results in different A and B matrices because these matrices are dependent of the control inputs (see Appendix IX).

In order to select the optimal control strategy, the 64 combination of control inputs, that defined 64 systems, were simulated using *lsim* function in Matlab (see Appendix IX for the Matlab script). The optimal control strategy was chosen by the following criteria:

1) The difference between the total mass of suspended particles in the concentrate and filtrate solution (Δm) obtained after one cycle should be maximal;

$$\Delta m = m_c - m_f = \int_0^{t_{cycle}} (Q_2(t) * S_2(t) - Q_1(t) * S_1(t))dt \quad (31)$$

2) The total mass of suspended particles in the filtrate solution (m_f) after one cycle should be minimal. The desired value is zero. As can be seen from equation 32, the total mass of the filtrate will be equal to zero in two cases, when the filtrate flow rate is zero all the time ($Q_1(t) = 0$) and when the concentration of particles is zero all the time($S_1(t) = 0$). If the filtrate flow rate is equal to zero all the time this means that the volume of filtrate solution is also zero ($V_f = 0$), in other words there is no production of filtrate solution. Consequently, in order to ensure that there is production of filtrate solution, its volume should be different from zero. As a result, the second criterion is: the total mass of suspended particles in the filtrate solution (m_f) after one cycle should be minimal and the volume of filtrate solution should be different from zero.

$$m_f = \int_0^{t_{cycle}} Q_1(t) * S_1(t)\, dt \quad (32)$$

3) The energy used during the process should be minimal.

Figure 15 shows the first two criteria as a function of the control strategies. According to the first criterion – there are eight combination of control inputs, which give the highest difference between the total mass of suspended particles in the concentrate and filtrate solution obtained after one cycle (see figure 15 – blue line). Taking into account the second criterion (see figure 15 –green line) the number of combinations are reduced from eight to two. These two combinations, namely 20th and 52nd, give the highest difference between the total mass of suspended particles in the concentrate and filtrate solution as well as the lowest total mass of suspended particles in filtrate solution after one cycle. Between these two combinations, the optimal one is chosen according to the third criterion. The only difference between these two combinations is the time when the transducer is working. In the 20th combination the transducer is switched on during the whole cycle (during both periods). However, in 52nd combination the transducer is working only during the short period. Therefore, the 52nd combination is more energy efficient that 20th and it represent the best control strategy. All eight combination, obtained according to the first criterion as well as all the three criteria are shown in table 3.

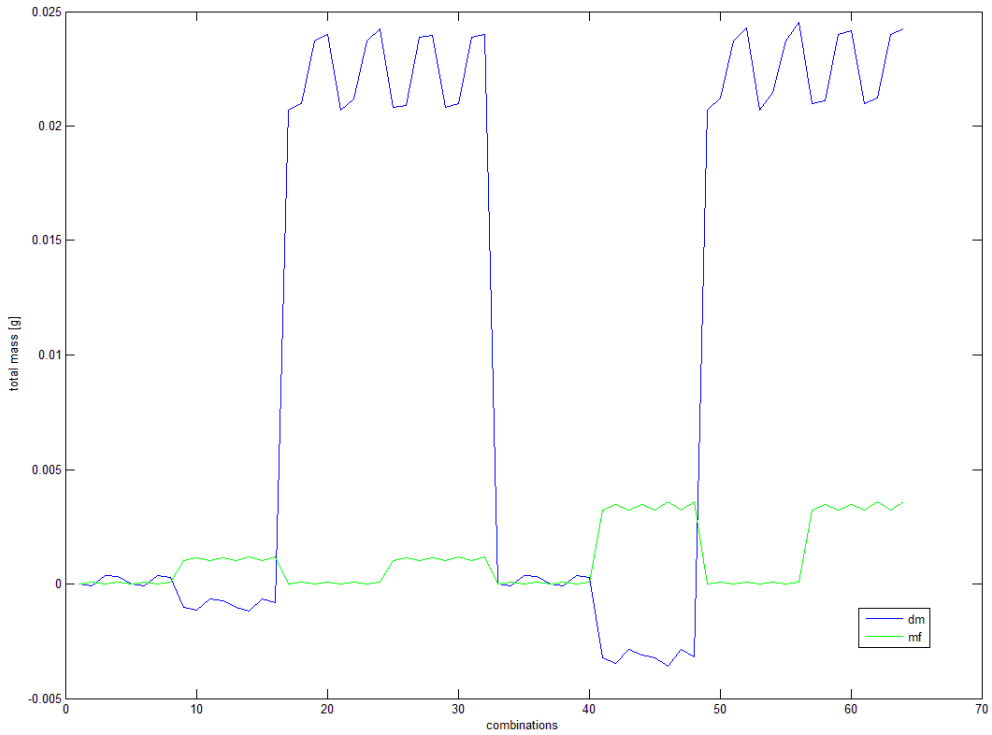

Figure 15 Performance index of all 64 control strategies

The optimal control strategy which gives the maximal difference between the total mass of suspended particles in concentrate and filtrate solution as well as minimum total mass of suspended particles in filtrate solution and uses minimum amount of energy is the 52nd. It consists of short period during which the transducer and both pumps are working and long period during which only pump 2 is working.

Table 3 Eight combinations of control inputs, which give the highest difference between the total mass of suspended particles in the concentrate and filtrate solution obtained after one cycle

Number of combination	Criterion 1 Δm [g] 10^{-2}	Criterion 2 m_f [g]	Criterion 3				
			period	α	Q_1 [ml/s]	Q_2 [ml/s]	V_f [ml]
20	2.4013	**$6.58*10^{-5}$**	Short-3s	1	0.46	1.38	1.38
			Long-30s	1	0	1.38	
24	2.4242	$1.01*10^{-4}$	Short-3s	0	0.46	1.38	1.38
			Long-30s	1	0	1.38	
28	2.3957	$1.13*10^{-3}$	Short-3s	1	0.46	1.38	15.18
			Long-30s	1	0.46	1.38	
32	2.4007	$1.20*10^{-3}$	Short-3s	0	0.46	1.38	15.18
			Long-30s	1	0.46	1.38	
52	2.4278	**$6.58*10^{-5}$**	Short-3s	**1**	**0.46**	**1.38**	**1.38**
			Long-30s	**0**	**0**	**1.38**	
56	2.4534	$1.01*10^{-4}$	Short-3s	0	0.46	1.38	1.38
			Long-30s	0	0	1.38	
60	2.4165	$3.49*10^{-3}$	Short-3s	1	0.46	1.38	15.18
			Long-30s	0	0.46	1.38	
64	2.4263	$3.60*10^{-3}$	Short-3s	0	0.46	1.38	15.18
			Long-30s	0	0.46	1.38	

4.3.2. Simulation of the controlled system

The output behaviour of the system controlled by the optimal control strategy is simulated over period of one (33 s) and ten cycles (330 s) using the estimated values of the parameters (see table 3, control strategy 52). The outputs of the systems are the three states – the concentrations of suspended particles in the three compartments (see Appendix X for the Matlab script). Figure 16 and 17 shows the dynamics of the controlled system with time step of 0.1 seconds during one and then cycles, respectively.

The behaviour of the controlled system, which is simulated over one cycle, was as expected. The cycle starts with short period of 3 s, during which the transducer is switched on and both pumps are working. Therefore, the concentrations of suspended particles in compartment 1 (blue line in figure 16) and in compartment 2 (green line in figure 16) was expected to increase due to the incoming portions of stock solution. As can be seen from figure 16 these expectations are confirmed. Moreover, the concentration in the third compartment (red line in figure 16) also increases during this period. This was also expected because the concentration reaction of suspended particles from compartment 1 to compartment 3 has constant rate due to the fixed ultrasonic field and because of the constant income of new portions of stock solution to compartment 1 due to the fixed filtrate flow rate.

However, the short period is followed by long period during which only pump 2 is working. The expected decrease in S_3 is observed, too (see figure 16). This decrease is caused by reverse concentration reaction, which occurs during the long period when the transducer is switched off. As

a result, particles from compartment 3 are released to compartment 1. It can also be seen from figure 16 that S_1 decreases during the long period and will eventually reach zero. This result was also expected because pump 1 is not working during the long period. Hence, new portions of stock solution are not coming to the first compartment. Moreover, since the transducer as well as pump 1 is switched off during the long period, no ultrasonic field is generated. So, only settling reaction of the particles from compartment 1 to compartment 3 occurs, which results in decreasing of S_1. When all particles from compartment 1 are settled, S_1 become zero.

S_2 increases during the long period as can be seen in figure 16. This is also expected result because pump 2 is working during the period and the settling reaction takes place.

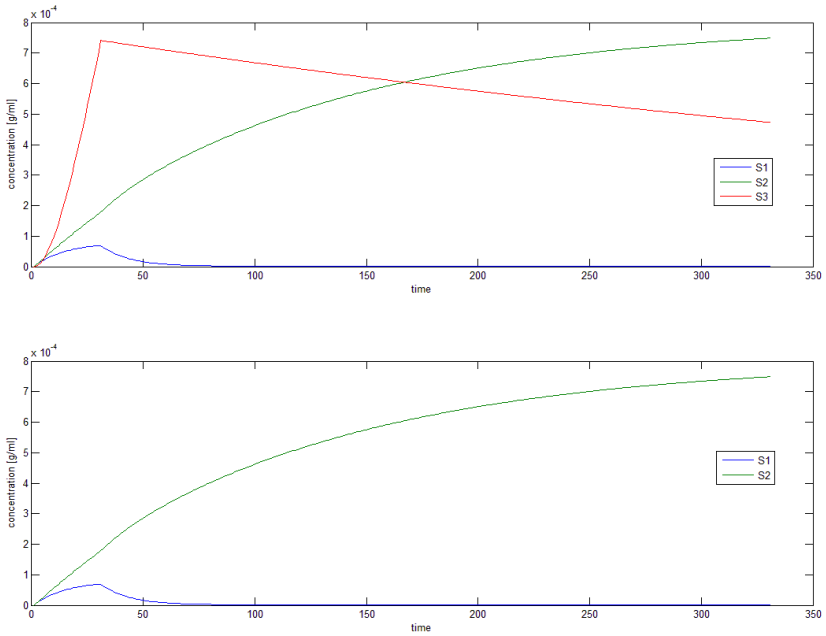

Figure 16 Simulation of the controlled system behaviour over 1 cycle

The described changes in the three concentrations during one cycle are repeated, when the system behaviour is simulated over ten cycles (see figure 17). The concentration in compartment 1 reaches its steady state value every cycle during the off-period, which is the long one. Similarly, the concentration in compartment 2 reaches its steady state value after the second cycle, again during its off-period (see figure 17). However, because not all particles from compartment 3 are released to compartment 1 during the off-periods, S_3 does not reach zero every off-period and thus it starts the on-period from value different from zero, which increases after every cycle. The reason for that is the estimated value of the reverse concentration reaction coefficient (k_3), which is very small (see section *4.2.4 Estimation of* k_3). Consequently, the reverse concentration reaction is slow which is in contrast with the expectations. Therefore, better estimation of k_3 has to be considered from new experiments.

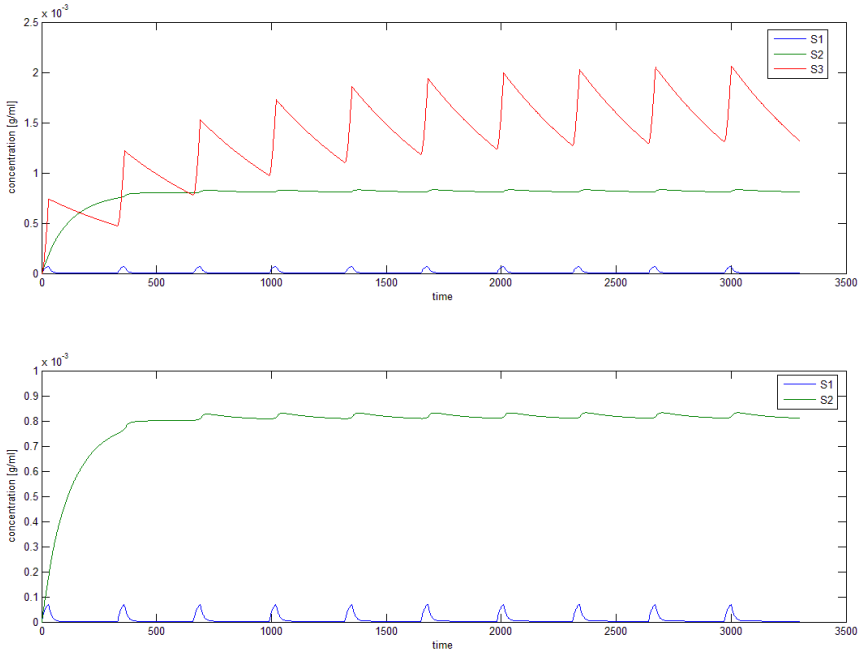

Figure 17 Simulation of the controlled system behaviour over 10 cycles

4.3.3. Comparison between the optimal control strategy and the current one

The main difference between the optimal control strategy and the current one, which was used in the experiments, is the time during which the transducer is on and off. The order of the on- and off-periods also differs (see Table 4). During the experiments the transducer was firstly switched off for short period of 3 seconds and then it was switched on for long period of 30 seconds. In contrast, the optimal control strategy starts with short period of 3 seconds, during which the transducer is switched on, and then it continues with long period of 30 seconds, during which the transducer is switched off. In both cases, pump 1 is connected with the transducer. As a result, during the on-periods both pumps and the transducer are working and during the off-periods only pump 2 is working.

Table 4 Comparison between the optimal control strategy and the current one

Strategy	Criterion 1 Δm [g] 10^{-2}	Criterion 2 m_f [g]	Criterion 3				
			period	α	Q_1 [ml/s]	Q_2 [ml/s]	V_f [ml]
Current	2.3881	$1.03*10^{-3}$	Short-3s –off	0	0	1.38	13.8
			Long-30s - on	1	0.46	1.38	
Optimal control	2.4278	$6.58*10^{-5}$	Short-3s - on	1	0.46	1.38	1.38
			Long-30 s -off	0	0	1.38	

From this comparison it can be concluded that the time needed for concentration of the particles by ultrasonic field is less than the time need for settling of these particles.

5. Conclusion

The behavior of the suspended particles during the ultrasound enhanced sedimentation was examined during this study. The particles behave as the theory predicts. They are concentrated by acoustic forces when the ultrasonic field is generated. However, when the ultrasonic field is switched off, the particles are no longer held by the acoustic field. Consequently, they settle down because of the gravity force.

A model of the commercially available device BioSep, which employs the ultrasound enhanced sedimentation, was developed. The choices for system boundaries and variables as well as all assumptions that were made during the modelling were described. Subsequently, the system properties were examined.

The unknown parameters in the model were estimated using steady state analysis and dynamic data from experiments. Then the behavior of the linearized system around steady state was simulated. The results showed that the on-line turbidity meter, which was used for dynamic measurements, is not so sensitive and it cannot detect all changes, which were expected. Therefore, more accurate sensor should be considered for the dynamic measurements and further experiments for parameter estimation should be performed, especially for k_3.

The optimal switching open-loop control strategy for the BioSep was designed such that high separation efficiency can be achieved. In the current study the optimal control strategy is in terms of maximal difference between the total mass of suspended particles in concentrate and filtrate solution as well as minimum total mass of suspended particles in filtrate solution and minimum amount of energy. This strategy consists of short period during which the transducer and both pumps are working and long period during which only pump 2 is working.

6. Recommendations

Because of the fact that parameters in the model play an important role for the selection of control strategy, better estimation of them, especially of k_3, using more accurate on-line measurement devices should be realized. Moreover, the model should be validated and the control strategy should be implemented in practise. On the other hand, a closed-loop control can be considered as well for better performance.

References

1. Svarovsky, L., *Solid-liquid separation*. fourth ed2001: Elsevier Ltd.
2. Tarleton, E.S., *The role of Field-assisted techniques in solid/liquid separation.* Filtration & Separation, 1992. **29**(3): p. 246-238.
3. Gröschl, M., *Ultrasonic Separation of Suspended Particles - Part I: Fundamentals.* Acustica, 1998. **84**(3): p. 432-447.
4. Gröschl, M., *Ultrasonic Separation of Suspended Particles - Part II: Design and Operation of Separation Devices.* Acta Acustica united with Acustica, 1998. **84**(4): p. 632-642.
5. Hill, M., et al., *Ultrasonic Particle Manipulation Microfluidic Technologies for Miniaturized Analysis Systems*, 2007, Springer US. p. 357-392.
6. Schram, C.J., *The manipulation of particles in an acoustic field*, in *Advances in Sonochemistry* T.J. Mason, Editor 1991, JAI Press: London. p. 293-322.
7. Gröschl, M., et al., *Ultrasonic Separation of Suspended Particles - Part III: Application in Biotechnology.* Acta Acustica united with Acustica, 1998. **84**(5): p. 815-822.
8. Coakley, W.T., *Ultrasonic separations in analytical biotechnology.* Trends in Biotechnology, 1997. **15**(12): p. 506-511.
9. Doblhoff-Dier, O., et al., *A Novel Ultrasonic Resonance Field Device for the Retention of Animal Cells.* Biotechnology Progress, 1994. **10**(4): p. 428-432.
10. Böhm, H., et al., *Viability of plant cell suspensions exposed to homogeneous ultrasonic fields of different energy density and wave type.* Ultrasonics, 2000. **38**(1–8): p. 629-632.
11. Wang, Z., et al., *Retention and Viability Characteristics of Mammalian Cells in an Acoustically Driven Polymer Mesh.* Biotechnology Progress, 2004. **20**(1): p. 384-387.
12. Bosma, R., et al., *Ultrasound, a new separation technique to harvest microalgae.* Journal of Applied Phycology, 2003. **15**(2): p. 143-153.
13. Dyson, M., B. Woodward, and J.B. Pond, *Flow of Red Blood Cells stopped by Ultrasound.* 1971. **232**(5312): p. 572-573.
14. Baker, N.V., *Segregation and Sedimentation of Red Blood Cells in Ultrasonic Standing Waves.* 1972. **239**(5372): p. 398-399.
15. Gherardini, L., et al., *A new immobilisation method to arrange particles in a gel matrix by ultrasound standing waves.* Ultrasound in Medicine & Biology, 2005. **31**(2): p. 261-272.
16. Cousins, C.M., et al., *Plasma preparation from whole blood using ultrasound.* Ultrasound in Medicine and Biology, 2000. **26**(5): p. 881-888.
17. Cousins, C.M., et al., *Clarification of plasma from whole human blood using ultrasound.* Ultrasonics, 2000. **38**(1–8): p. 654-656.

Appendix I State space representation of the BioSep's model

States variables: $x_1 = S_1(t);\ x_2 = S_2(t);\ x_3 = S_3(t);$

Inputs: $u_1 = Q_1;\ u_2 = Q_2;\ u_3 = S_{in};\ u_4 = \alpha;$

$u_1 = Q_1,\ u_2 = Q_2\ and\ u_4 = \alpha$ are control inputs; $u_3 = S_{in}$ is disturbance input.

Parameters: $p_1 = k_1;\ p_2 = k_2;\ p_3 = k_3;\ p_4 = k_4;\ p_5 = V_1; p_6 = V_2; p_7 = V_3;$ (assuming that V_1, V_2, V_3 are constant);

Outputs: $y_1 = S_1(t) = x_1;\ y_2 = S_2(t) = x_2;\ y_3 = S_3(t) = x_3$

The general form of state space representation of the BioSep's model is given by state equation and output equation:

State equation:

$$\dot{\mathrm{X}} = \boldsymbol{f}(\boldsymbol{x},\boldsymbol{u},\boldsymbol{p}) = \begin{pmatrix} \frac{dx_1}{dt} \\ \frac{dx_2}{dt} \\ \frac{dx_3}{dt} \end{pmatrix} = \begin{pmatrix} \frac{u_1 * u_3}{p_5} - \frac{u_1 * x_1}{p_5} - u_4 * p_1 * x_1 - \frac{p_2 * x_1}{u_1 + p_4} + \frac{(1-u_4) * p_3 * p_7 * x_3}{p_5} \\ \frac{u_2 * u_3}{p_6} - \frac{u_2 * x_2}{p_6} + \frac{p_2 * p_5 * x_1}{p_6 * (u_1 + p_4)} \\ \frac{u_4 * p_1 * p_5 * x_1}{p_7} - (1-u_4) * p_3 * x_3 \end{pmatrix} (I.1)$$

Output equation:

$$\boldsymbol{y} = \boldsymbol{g}(\boldsymbol{x},\boldsymbol{u},\boldsymbol{p}) = \begin{pmatrix} y_1 \\ y_2 \\ y_3 \end{pmatrix} = \begin{pmatrix} x_1 \\ x_2 \\ x_3 \end{pmatrix} (I.2)$$

A linearized version of the BioSep model is given by:

$$\Delta\dot{x} = A * \Delta x + B * \Delta u \ \ (I.3)$$

$$\Delta y = C * \Delta x + D * \Delta u \ \ (I.4)$$

With A, B, C and D potentially time-varying matrices.

There are three states variables; consequently, the system matrix (A) of the linearized system around steady state is 3x3 matrix and is given by:

$$A = \frac{\partial f(x,u,p)}{\partial x} = \begin{pmatrix} -\frac{u_1}{p_5} - u_4 * p_1 - \frac{p_2}{u_1 + p_4} & 0 & \frac{(1-u_4) * p_3 * p_7}{p_5} \\ \frac{p_2 * p_5}{p_6 * (u_1 + p_4)} & -\frac{u_2}{p_6} & 0 \\ \frac{u_4 * p_1 * p_5}{p_7} & 0 & -(1-u_4) * p_3 \end{pmatrix}_{u=u_{ss}} \quad (I.5)$$

Where $u = [\,u_1\ \ u_2\ \ u_3\ \ u_4]^T$ is the input vector and u_{ss} denotes steady states of the inputs.

The input matrix (B) of the linearized system around steady state has dimension 3x4 due to the fact that there are three states variables and four inputs.

$$B = \frac{\partial f(x,u,p)}{\partial u} = \begin{pmatrix} \frac{u_3}{p_5} - \frac{x_1}{p_5} + \frac{p_2 * x_1}{(u_1 + p_4)^2} & 0 & \frac{u_1}{p_5} & -p_1 * x_1 - \frac{p_3 * p_7 * x_3}{p_5} \\ -\frac{p_2 * p_5 * x_1}{p_6 * (u_1 + p_4)^2} & \frac{u_3}{p_6} - \frac{x_2}{p_6} & \frac{u_2}{p_6} & 0 \\ 0 & 0 & 0 & \frac{p_1 * p_5 * x_1}{p_7} + p_3 * x_3 \end{pmatrix}_{\substack{u=u_{ss} \\ x=x_{ss}}} \quad (I.6)$$

Where $x = [\ x\ \ x_2\ x_3\ ]^T$ is the state vector and x_{ss} denotes steady states of the states variables.

The dimension of the observation matrix (C), called also output matrix, of the linearized system is 3x3 because the number of outputs as well as the number of states variables are three.

$$C = \frac{\partial g(x,u,p)}{\partial x} = \begin{pmatrix} 1 & 0 & 0 \\ 0 & 1 & 0 \\ 0 & 0 & 1 \end{pmatrix} (I.7)$$

There are three outputs and four inputs; therefore, the feed-through matrix (D) of the linearized system has dimension 3x4.

$$D = \frac{\partial g(x,u,p)}{\partial u} = \begin{pmatrix} 0 & 0 & 0 & 0 \\ 0 & 0 & 0 & 0 \\ 0 & 0 & 0 & 0 \end{pmatrix} (I.8)$$

Appendix II System linearization

In general the state space form of BioSep's model is given by the state equation and the output equation.

State equation:

$$\dot{S} = \begin{pmatrix} \frac{dS_1}{dt} \\ \frac{dS_2}{dt} \\ \frac{dS_3}{dt} \end{pmatrix} = \begin{pmatrix} \frac{Q_1 * S_{in}}{V_1} - \frac{Q_1 * S_1}{V_1} + \frac{(1-\alpha) * k_3 * S_3 * V_3}{V_1} - \alpha * k_1 * S_1 - \frac{k_2 * S_1}{Q_1 + k_4} \\ \frac{Q_2 * S_{in}}{V_2} - \frac{Q_2 * S_2}{V_2} + \frac{k_2 * S_1 * V_1}{V_2 * (Q_1 + k_4)} \\ \frac{\alpha * k_1 * S_1 * V_1}{V_3} - (1-\alpha) * k_3 * S_3 \end{pmatrix} (II.1)$$

Output equation:

$$S = \begin{pmatrix} S_1 \\ S_2 \\ S_3 \end{pmatrix} (II.2)$$

Where the state variables, inputs, outputs and parameters are:

States variables: $x_1 = S_1(t);\ x_2 = S_2(t);\ x_3 = S_3(t);$

Inputs: $u_1 = Q_1;\ u_2 = Q_2;\ u_3 = S_{in};\ u_4 = \alpha;$

$u_1 = Q_1,\ u_2 = Q_2\ and\ u_4 = \alpha$ are control inputs; $u_3 = S_{in}$ is disturbance input.

Parameters: $p_1 = k_1;\ p_2 = k_2;\ p_3 = k_3;\ p_4 = k_4;\ p_5 = V_1; p_6 = V_2; p_7 = V_3;$

Outputs: $y_1 = S_1(t) = x_1;\ y_2 = S_2(t) = x_2;\ y_3 = S_3(t) = x_3$

Then, the state equation and output equation can be written as following:

State equation:

$$\dot{X} = \boldsymbol{f}(\boldsymbol{x}, \boldsymbol{u}, \boldsymbol{p}) = \begin{pmatrix} \frac{dx_1}{dt} \\ \frac{dx_2}{dt} \\ \frac{dx_3}{dt} \end{pmatrix} = \begin{pmatrix} \frac{u_1 * u_3}{p_5} - \frac{u_1 * x_1}{p_5} - u_4 * p_1 * x_1 - \frac{p_2 * x_1}{u_1 + p_4} + \frac{(1-u_4) * p_3 * p_7 * x_3}{p_5} \\ \frac{u_2 * u_3}{p_6} - \frac{u_2 * x_2}{p_6} + \frac{p_2 * p_5 * x_1}{p_6 * (u_1 + p_4)} \\ \frac{u_4 * p_1 * p_5 * x_1}{p_7} - (1-u_4) * p_3 * x_3 \end{pmatrix} (II.3)$$

Output equation:

$$\boldsymbol{y} = \boldsymbol{g}(\boldsymbol{x}, \boldsymbol{u}, \boldsymbol{p}) = \begin{pmatrix} y_1 \\ y_2 \\ y_3 \end{pmatrix} = \begin{pmatrix} x_1 \\ x_2 \\ x_3 \end{pmatrix} (II.4)$$

Due to the fact that transducer coefficient (α) has two values, two cases – when the transducer is switched on ($\alpha = 1$) and when it is switched off ($\alpha = 0$), are analyzed separately. Thus, the number of inputs decreases with one in each case. In the general case there are four inputs. However, in both cases, which are considered below, the inputs are three.

Case I: when the transducer is on, transducer coefficient is equal to 1 ($\alpha = 1$)

States variables: $x_1 = S_1(t);\ x_2 = S_2(t);\ x_3 = S_3(t);$

Inputs: $u_1 = Q_1;\ u_2 = Q_2;\ u_3 = S_{in};$

$u_1 = Q_1,\ u_2 = Q_2$ are control inputs; $u_3 = S_{in}$ is disturbance input.

Parameters: $p_1 = k_1;\ p_2 = k_2;\ p_3 = k_3;\ p_4 = k_4;\ p_5 = V_1; p_6 = V_2; p_7 = V_3;$

Outputs: $y_1 = S_1(t) = x_1;\ y_2 = S_2(t) = x_2;\ y_3 = S_3(t) = x_3$

When the transducer is switched on, II.1 becomes:

$$\dot{S_1} = \begin{pmatrix} \frac{dS_1}{dt} \\ \frac{dS_2}{dt} \\ \frac{dS_3}{dt} \end{pmatrix} = \begin{pmatrix} \frac{Q_1 * S_{in}}{V_1} - \frac{Q_1 * S_1}{V_1} - k_1 * S_1 - \frac{k_2 * S_1}{Q_1 + k_4} \\ \frac{Q_2 * S_{in}}{V_2} - \frac{Q_2 * S_2}{V_2} + \frac{k_2 * S_1 * V_1}{V_2 * (Q_1 + k_4)} \\ \frac{k_1 * S_1 * V_1}{V_3} \end{pmatrix} \quad (II.5)$$

II.2 is independent of the transducer coefficient; so, the output equation in this case is still the same as in the general case.

The system is non-linear but it is linearized around steady state. As a result, the following A_1, B_1, C_1 and D_1 matrices of the linearized system are obtained:

$$A_1 = \begin{pmatrix} -\frac{Q_1}{V_1} - k_1 - \frac{k_2}{Q_1 + k_4} & 0 & 0 \\ \frac{k_2 * V_1}{V_2 * (Q_1 + k_4)} & -\frac{Q_2}{V_2} & 0 \\ \frac{k_1 * V_1}{V_3} & 0 & 0 \end{pmatrix}_{\substack{Q_1 = Q_{1sson} \\ Q_2 = Q_{2sson}}} \quad (II.6);$$

$$B_1 = \begin{pmatrix} \frac{S_{in}}{V_1} - \frac{S_1}{V_1} + \frac{k_2 * S_1}{(Q_1 + k_4)^2} & 0 & \frac{Q_1}{V_1} \\ -\frac{k_2 * S_1 * V_1}{V_2 * (Q_1 + k_4)^2} & \frac{S_{in}}{V_2} - \frac{S_2}{V_2} & \frac{Q_2}{V_2} \\ 0 & 0 & 0 \end{pmatrix}_{\substack{Q_1 = Q_{1sson} \\ Q_2 = Q_{2sson}}} \quad (II.7);$$

$$C_1 = \begin{pmatrix} 1 & 0 & 0 \\ 0 & 1 & 0 \\ 0 & 0 & 1 \end{pmatrix} (II.8); \quad D_1 = \begin{pmatrix} 0 & 0 & 0 \\ 0 & 0 & 0 \\ 0 & 0 & 0 \end{pmatrix} (II.9)$$

Case II: when the transducer is off, transducer coefficient is equal to 0 ($\alpha = 0$)

States variables: $x_1 = S_1(t);\ x_2 = S_2(t);\ x_3 = S_3(t);$

Inputs: $u_1 = Q_1;\ u_2 = Q_2;\ u_3 = S_{in};$

$u_1 = Q_1,\ u_2 = Q_2$ are control inputs; $u_3 = S_{in}$ is disturbance input.

Parameters: $p_1 = k_1;\ p_2 = k_2;\ p_3 = k_3;\ p_4 = k_4;\ p_5 = V_1; p_6 = V_2; p_7 = V_3;$

Outputs: $y_1 = S_1(t) = x_1;\ y_2 = S_2(t) = x_2;\ y_3 = S_3(t) = x_3$

When the transducer is switched off, II.1 becomes:

$$\dot{S_2} = \begin{pmatrix} \frac{dS_1}{dt} \\ \frac{dS_2}{dt} \\ \frac{dS_3}{dt} \end{pmatrix} = \begin{pmatrix} \frac{Q_1 * S_{in}}{V_1} - \frac{Q_1 * S_1}{V_1} + \frac{k_3 * S_3 * V_3}{V_1} - \frac{k_2 * S_1}{Q_1 + k_4} \\ \frac{Q_2 * S_{in}}{V_2} - \frac{Q_2 * S_2}{V_2} + \frac{k_2 * S_1 * V_1}{V_2 * (Q_1 + k_4)} \\ -k_3 * S_3 \end{pmatrix} (II.10)$$

II.2 is independent of the transducer coefficient; so, the output equation in this case is still the same as in the general case as well as in the first case when the transducer is switched on.

The system is non-linear but it is linearized around steady state. As a result, the following A_2, B_2, C_2 and D_2 matrices of the linearized system are obtained:

$$A_2 = \begin{pmatrix} -\frac{Q_1}{V_1} - \frac{k_2}{Q_1 + k_4} & 0 & \frac{k_3 * V_3}{V_1} \\ \frac{k_2 * V_1}{V_2 * (Q_1 + k_4)} & -\frac{Q_2}{V_2} & 0 \\ 0 & 0 & -k_3 \end{pmatrix}_{\substack{Q_1 = Q_{1ssoff} \\ Q_2 = Q_{2ssoff}}} (II.11);$$

$$B_2 = \begin{pmatrix} \frac{S_{in}}{V_1} - \frac{S_1}{V_1} + \frac{k_2 * S_1}{(Q_1 + k_4)^2} & 0 & \frac{Q_1}{V_1} \\ -\frac{k_2 * S_1 * V_1}{V_2 * (Q_1 + k_4)^2} & \frac{S_{in}}{V_2} - \frac{S_2}{V_2} & \frac{Q_2}{V_2} \\ 0 & 0 & 0 \end{pmatrix}_{\substack{Q_1 = Q_{1ssoff} \\ Q_2 = Q_{2ssoff}}} (II.12)$$

$$C_2 = \begin{pmatrix} 1 & 0 & 0 \\ 0 & 1 & 0 \\ 0 & 0 & 1 \end{pmatrix} (II.13); \quad D_2 = \begin{pmatrix} 0 & 0 & 0 \\ 0 & 0 & 0 \\ 0 & 0 & 0 \end{pmatrix} (II.14)$$

The C and D matrices in both cases are the same because the output equation (II.2) is independent of the value of transducer coefficient (α).

Appendix III Matlab script for the system properties - observability and controllability

```
% symbolically testing the properties of the linearized system
syms V1 V2 V3 Q1 Q2 Sin S1 S2 k1 k2 k3 k4 a;

%1st case - transducer is on alpha=1
A1=[ -Q1/V1-k1-k2/(Q1+k4) 0 0; k2*V1/(V2*(Q1+k4)) -Q2/V2 0; k1*V1/V3 0 0]
B1=[ Sin/V1-S1/V1+(k2*S1)/((Q1+k4)^2) 0 Q1/V1; -(k2*S1*V1)/(V2*(Q1+k4)^2)
(Sin-S2)/V2 Q2/V2; 0 0 0]
C1=eye(3)

% controllability
CM1=[B1 A1*B1 (A1^2)*B1];
rc1=rank(CM1);
[nc1,mc1]=size(CM1);
if nc1==rc1
     disp('controllable')
else disp('uncontrollable')
end

% observability
OM1=[C1 C1*A1 C1*(A1^2)]';
ro1=rank(OM1);
[no1,mo1]=size(OM1);
if mo1==ro1
     disp('observable')
else disp('unobservable')
end

%2nd case - transducer is on alpha=0
A2=[ -Q1/V1-k2/(Q1+k4) 0 k3*V3/V1; k2*V1/(V2*(Q1+k4)) -Q2/V2 0; 0 0 -k3]
B2=[ Sin/V1-S1/V1+(k2*S1)/((Q1+k4)^2) 0 Q1/V1; -(k2*S1*V1)/(V2*(Q1+k4)^2)
(Sin-S2)/V2 Q2/V2; 0 0 0]
C2=eye(3)

% controllability
CM2=[B2 A2*B2 (A2^2)*B2];
rc2=rank(CM2);
[nc2,mc2]=size(CM2);
if nc2==rc2
     disp('controllable')
else disp('non-controllable')
end

% observability
OM2=[C2 C2*A2 C2*(A2^2)]';
ro2=rank(OM2);
[no2,mo2]=size(OM2);
if mo2==ro2
     disp('observable')
else disp('non-observable')
end
```

Appendix IV Steady state analysis

If the system is at steady state, all derivatives of the states with respect to time are zero.

$$\frac{dS_1}{dt} = 0 \;\; ; \frac{dS_2}{dt} = 0 \;\; ; \frac{dS_3}{dt} = 0$$

Hence, the equation 1 of the BioSep model (see section *3.1.1 BioSep Model*) becomes IV.2.

$$0 = Q_1 * S_{in} - Q_1 * S_{1ss} + (1-\alpha) * k_3 * S_{3ss} * V_3 - \alpha * k_1 * S_{1ss} * V_1 - \frac{k_2 * S_{1ss} * V_1}{Q_1 + k_4} \quad (IV.1)$$

$$\boldsymbol{(1-\alpha) * k_3 * S_{3ss} * V_3 - \alpha * k_1 * S_{1ss} * V_1 - \frac{k_2 * S_{1ss} * V_1}{Q_1 + k_4} = Q_1 * (S_{1ss} - S_{in})} \quad \boldsymbol{(IV.2)}$$

Furthermore, the equation 2 of the BioSep model (see section *3.1.1 BioSep Model*) becomes IV.4:

$$0 = Q_2 * S_{in} - Q_2 * S_{2ss} + \frac{k_2 * S_{1ss} * V_1}{Q_1 + k_4} \quad (IV.3)$$

$$\boldsymbol{\frac{k_2 * S_{1ss} * V_1}{Q_1 + k_4} = Q_2 * (S_{2ss} - S_{in})} \quad \boldsymbol{(IV.4)}$$

Moreover, equation 3 of the BioSep model (see section *3.1.1 BioSep Model*) becomes the following:

$$\boldsymbol{\alpha * k_1 * S_{1ss} * V_1 - (1-\alpha) * k_3 * S_{3ss} * V_3 = 0}^{2} \quad \boldsymbol{(IV.5)}$$

As a result, the following linear regression is obtained:

$$\begin{pmatrix} -\alpha * S_{1ss} * V_1 & -S_{1ss} * V_1 & (1-\alpha) * S_{3ss} * V_3 \\ 0 & S_{1ss} * V_1 & 0 \\ \alpha * S_{1ss} * V_1 & 0 & -(1-\alpha) * S_{3ss} * V_3 \end{pmatrix} \begin{pmatrix} k_1 \\ \frac{k_2}{Q_1+k_4} \\ k_3 \end{pmatrix} = \begin{pmatrix} Q_1 * (S_{1ss} - S_{in}) \\ Q_2 * (S_{2ss} - S_{in}) \\ 0 \end{pmatrix} (IV.6)$$

In order to simplify the analysis two cases for the transducer, when it is switched on ($\alpha = 1$) and when it is switched off ($\alpha = 0$), are analyzed separately.

[2] Equation IV.5 holds only when the transducer is switched off (α=0) because only in this case a steady state for the concentration in compartment 3 (S_{3ss}) is possible. In this case equation IV.5 becomes:

$$-k_3 * S_{3ssoff} * V_3 = 0 \quad (IV.5.1)$$

When the transducer is switched on (α=1), equation IV.5 does not hold because steady state of S_{3ss} cannot be achieved. The concentration of suspended particles in compartment 3 is expected to increase over the time due to the occurrence of the concentration reaction of particles between compartment 1 and compartment 3. Thus, the equation IV.5 becomes:

$$k_1 * S_{1sson} * V_1 = \frac{dS_3}{dt} \; (IV.5.2)$$

Case I: when the transducer is on, transducer coefficient is equal to 1 ($\alpha = 1$)

When the transducer is on, the linear regression (IV.6) becomes:

$$\begin{pmatrix} -S_{1sson} * V_1 & -S_{1sson} * V_1 \\ 0 & S_{1sson} * V_1 \end{pmatrix} \begin{pmatrix} k_1 \\ k_2 \\ \hline Q_1 + k_4 \end{pmatrix} = \begin{pmatrix} Q_1 * (S_{1sson} - S_{in}) \\ Q_2 * (S_{2sson} - S_{in}) \end{pmatrix} (IV.7)$$

Assuming that the filtrate flow rate is much higher than loss coefficient $(i.e.\ Q_1 \gg k_4)$, further simplification of IV.7 can be done:

$$\begin{pmatrix} -S_{1sson} * V_1 & -\dfrac{S_{1sson} * V_1}{Q_1} \\ 0 & \dfrac{S_{1sson} * V_1}{Q_1} \end{pmatrix} \begin{pmatrix} k_1 \\ k_2 \end{pmatrix} = \begin{pmatrix} Q_1 * (S_{1sson} - S_{in}) \\ Q_2 * (S_{2sson} - S_{in}) \end{pmatrix} (IV.8)$$

Consequently, the estimates of both parameters k_1 and k_2 can be found from the following expression after evaluating its right-hand side:

$$\begin{pmatrix} \widehat{k_1} \\ k_2 \end{pmatrix} = \begin{pmatrix} -S_{1sson} * V_1 & -\dfrac{S_{1sson} * V_1}{Q_1} \\ 0 & \dfrac{S_{1sson} * V_1}{Q_1} \end{pmatrix}^{-1} \begin{pmatrix} Q_1 * (S_{1sson} - S_{in}) \\ Q_2 * (S_{2sson} - S_{in}) \end{pmatrix} (IV.9)$$

The outcome is:

$$\begin{pmatrix} \widehat{\boldsymbol{k_1}} \\ \boldsymbol{k_2} \end{pmatrix} = \begin{pmatrix} -\dfrac{\boldsymbol{Q_1 * (S_{1sson} - S_{in}) + Q_2 * (S_{2sson} - S_{in})}}{\boldsymbol{S_{1sson} * V_1}} \\ \dfrac{\boldsymbol{Q_1 * Q_2 * (S_{2sson} - S_{in})}}{\boldsymbol{S_{1sson} * V_1}} \end{pmatrix} (\boldsymbol{IV.10})$$

$\widehat{k_1}$ can also be expressed as:

$$\widehat{\boldsymbol{k_1}} = -\frac{\boldsymbol{Q_1 * (S_{1sson} - S_{in})}}{\boldsymbol{S_{1sson} * V_1}} - \frac{\widehat{\boldsymbol{k_2}}}{\boldsymbol{Q_1}} (\boldsymbol{IV.11})$$

Case II: when the transducer is off, transducer coefficient is equal to 0 ($\alpha = 0$)

When the transducer is off, the transducer coefficient is equal to zero $(\alpha = 0)$ and the filtrate flow rate is also equal to zero $(Q_1 = 0)$. Thus, the linear regression (IV.6) becomes:

$$\begin{pmatrix} 0 & -S_{1ssoff} * V_1 & S_{3ssoff} * V_3 \\ 0 & S_{1ssof} * V_1 & 0 \\ 0 & 0 & -S_{3ssoff} * V_3 \end{pmatrix} \begin{pmatrix} k_1 \\ k_2 \\ \hline k_4 \\ k_3 \end{pmatrix} = \begin{pmatrix} 0 \\ Q_2 * (S_{2ssoff} - S_{in}) \\ 0 \end{pmatrix} (IV.12)$$

Estimate of k_4 can be found from the following equation:

$$S_{1ssoff} * V_1 * \frac{\widehat{k_2}}{\widehat{k_4}} = Q_2 * (S_{2ssoff} - S_{in}) (IV.13)$$

After reengagement, the following expression for $\widehat{k_4}$ is obtained:

$$\widehat{k_4} = \frac{S_{1ssoff} * V_1 * \widehat{k_2}}{Q_2 * (S_{2ssoff} - S_{in})} \ (IV.14)$$

After substituting $\widehat{k_2}$ in equation IV.14 the following expression for $\widehat{k_4}$ is obtained:

$$\widehat{k_4} = \frac{S_{1ssoff} * V_1 * \frac{Q_1 * Q_2 * (S_{2sson} - S_{in})}{S_{1sson} * V_1}}{Q_2 * \left(S_{2ssoff} - S_{in}\right)} \ (IV.15)$$

Although S_{3ss} exists in this case, it cannot be use for estimation of k_3 because the steady state value of concentration of suspended particles in compartment 3 during the off-period is expected to be zero. Therefore, the following equation always holds independently of k_3:

$$-k_3 * S_{3ssoff} * V_3 = 0 \ (IV.16)$$

Appendix V Determination of the pump rate of the stock solution

Assuming that there is another pump which determines the flow rate of stock solution in the current setting, its rate can be calculated as it is described below.

Case I: when the transducer is on, transducer coefficient is equal to 0 ($\alpha = 1$)

When the transducer is on, both pumps are working. Therefore, the flow rate of the incoming stock solution to the BioSep is given by the following equation:

$$Q_{in}(on) = Q_1 + Q_2 \quad (V.1)$$

Case II: when the transducer is off, transducer coefficient is equal to 0 ($\alpha = 0$)

When the transducer is off, only pump 2 is working. Therefore, the flow rate of the incoming stock solution to the BioSep is given by the following equation:

$$Q_{in}(off) = Q_2 \quad (V.2)$$

If the two cases are combined, the general expresion for the average flow rate of the stock solution during one cycle, consisting of on- and off- period, is obtained (eq. V.7).

$$Q_{in}(cycle) * t_{cycle} = Q_{in}(on) * t_{on} + Q_{in}(off) * t_{off} \quad (V.3)$$

$$Q_{in}(cycle) * t_{cycle} = (Q_1 + Q_2) * t_{on} + Q_2 * t_{off} \quad (V.4)$$

$$Q_{in}(cycle) * t_{cycle} = Q_1 * t_{on} + Q_2 * t_{on} + Q_2 * t_{off} \quad (V.5)$$

$$Q_{in}(cycle) * t_{cycle} = Q_1 * t_{on} + Q_2 * t_{cycle} \quad (V.6)$$

$$\boldsymbol{Q_{in}(cycle) = \frac{(Q_1 * t_{on} + Q_2 * t_{cycle})}{t_{cycle}}} \quad \boldsymbol{(V.7)}$$

If instead flow rates, pump rates are used in the equation V.7, it becomes:

$$\boldsymbol{Pr_{in}(cycle) = \frac{(Pr_1 * t_{on} + Pr_2 * t_{cycle})}{t_{cycle}}} \quad \boldsymbol{(V.8)}$$

Where, Pr_{in} is the pump rate of the pump, which determines the flow rate of the incoming stock solution, Pr_1 and Pr_2 are the pump rates of pump 1 and pump 2, which determine the filtrate flow rate and concentrate flow rate, respectively.

The stock solution's pump rate is calculated using equation V.8 When the pump rate of pump 1 and 2 are fixed (the rate of pump 1 is 2, the rate of pump 2 is 5) and duration of the off- and on -period is 3 s and 30 s, respectively; the rate of the pump for the stock solution is:

$$Pr_{in}(cycle) = \frac{2 * 30 + 5 * 33)}{33} = \ 6.8 \ (V.9)$$

Appendix VI Dynamics of S_{in}, S_1 and S_2 obtained from the experiments with 0.83 g/L starch solution

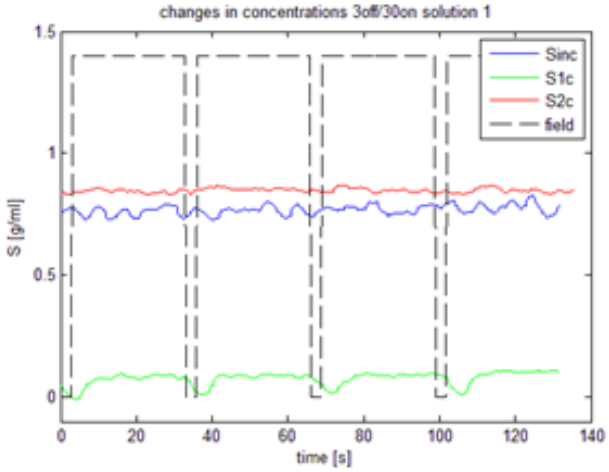

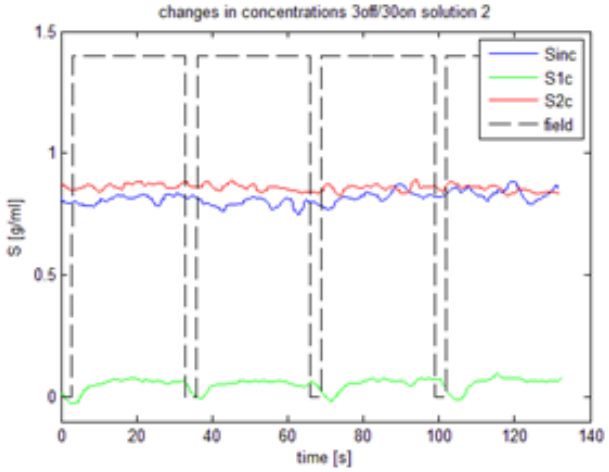

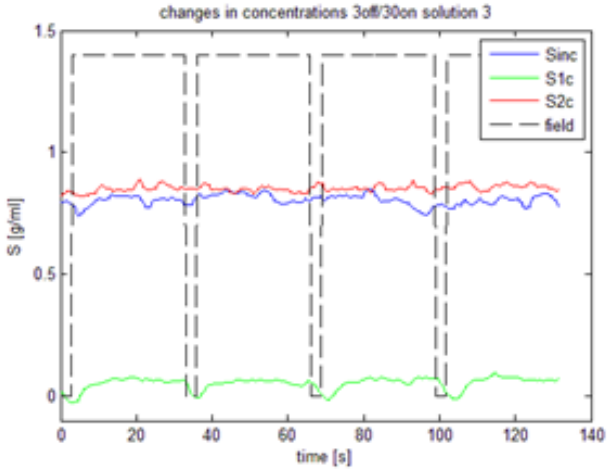

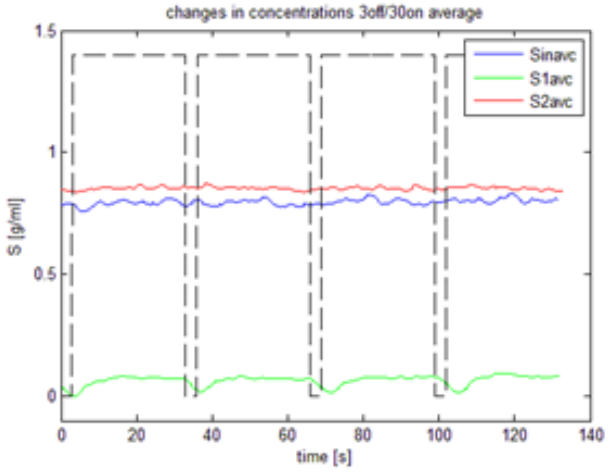

Appendix VII Changes in S_1 during the off-periods

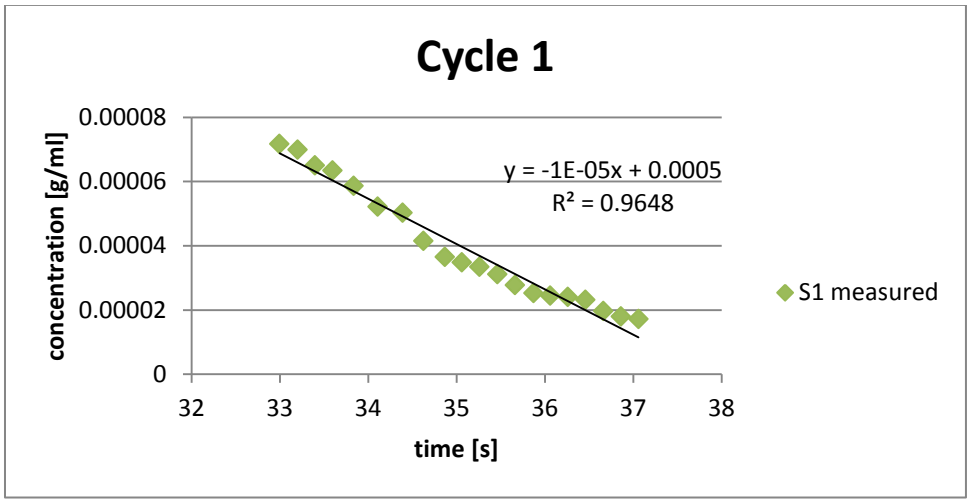

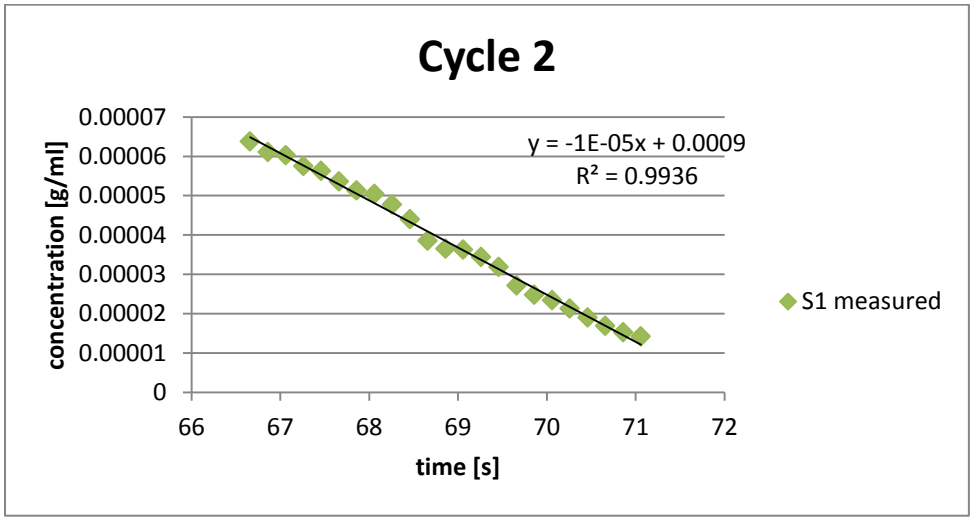

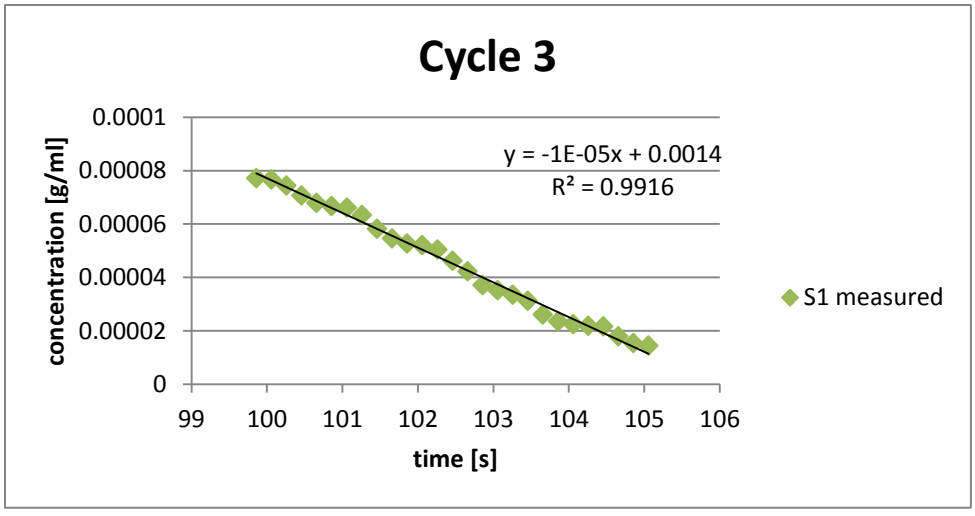

Appendix VIII Matlab script for the simulaton of BioSep

```
% Simulation of BioSep with estimated parameters
t1=0:.1:3; t2=0:0.1:30;
Sin=7.97/10000;
k1=0.534; k2=0.075; k3=0.015; k4=0.093;
Q1=0.46;Q2=1.38;
V1=6.36;V2=17;V3=0.64;
X0=zeros(3,1);
% alpha=0
A =[-Q1/V1-k2/(Q1+k4) 0 k3*V3/V1;(V1/V2)*(k2/(Q1+k4)) -Q2/V2 0; 0 0 -k3]
%alpha=1
A1=[-Q1/V1-k1-k2/(Q1+k4) 0 0;(V1/V2)*(k2/(Q1+k4)) -Q2/V2 0; k1*V1/V3 0 0]
B=[Q1/V1;Q2/V2;0]
C=eye(3)
D=zeros(3,1)
% creating an object G0 and G1 representing the continuous-time state-space
model;
G0=ss(A,B,C,D,'StateName',{'x1=S1 concentration in compartment 1';'x2=S2
concentration in compartment 2'; 'x3=S3 concentration in compartment
3'},'StateUnit',{'g/ml' ; 'g/ml'; 'g/ml'},'OutputName', {'y1=S1
concentration in compartment 1';'y2=S2 concentration in compartment 2';
'y3=S3 concentration in compartment 3'}, 'OutputUnit',{'g/ml' ; 'g/ml';
'g/ml'})  % when alpha=0, transducer 'off'
G1=ss(A1,B,C,D,'StateName',{'x1=S1 concentration in compartment 1';'x2=S2
concentration in compartment 2'; 'x3=S3 concentration in compartment
3'},'StateUnit',{'g/ml' ; 'g/ml'; 'g/ml'}, 'OutputName', {'y1=S1
concentration in compartment 1';'y2=S2 concentration in compartment 2';
'y3=S3 concentration in compartment 3'}, 'OutputUnit',{'g/ml' ; 'g/ml';
'g/ml'}) % when alpha=1, transducer 'on'
y=[]
% simulations
Y(1:31,1:3)=lsim(G0,[Sin*ones(length(t1),1)],t1,X0);
Y(31:331,1:3)=lsim(G1,[Sin*ones(length(t2),1)],t2,Y(31,:)'); %1 cycle
Y(331:361,1:3)=lsim(G0,[Sin*ones(length(t1),1)],t1,Y(331,:)');
Y(361:661,1:3)=lsim(G1,[Sin*ones(length(t2),1)],t2,Y(361,:)');%2 cycle
Y(661:691,1:3)=lsim(G0,[Sin*ones(length(t1),1)],t1,Y(661,:)');
Y(691:991,1:3)=lsim(G1,[Sin*ones(length(t2),1)],t2,Y(691,:)');%3 cycle
Y(991:1021,1:3)=lsim(G0,[Sin*ones(length(t1),1)],t1,Y(991,:)');
Y(1021:1321,1:3)=lsim(G1,[Sin*ones(length(t2),1)],t2,Y(1021,:)');%4 cycle
Y(1321:1351,1:3)=lsim(G0,[Sin*ones(length(t1),1)],t1,Y(1321,:)');
Y(1351:1651,1:3)=lsim(G1,[Sin*ones(length(t2),1)],t2,Y(1351,:)'); %5 cycle
Y(1651:1681,1:3)=lsim(G0,[Sin*ones(length(t1),1)],t1,Y(1651,:)');
Y(1681:1981,1:3)=lsim(G1,[Sin*ones(length(t2),1)],t2,Y(1681,:)'); %6 cycle
Y(1981:2011,1:3)=lsim(G0,[Sin*ones(length(t1),1)],t1,Y(1981,:)');
Y(2011:2311,1:3)=lsim(G1,[Sin*ones(length(t2),1)],t2,Y(2011,:)');%7 cycle
Y(2311:2341,1:3)=lsim(G0,[Sin*ones(length(t1),1)],t1,Y(2311,:)');
Y(2341:2641,1:3)=lsim(G1,[Sin*ones(length(t2),1)],t2,Y(2341,:)');%8 cycle
Y(2641:2671,1:3)=lsim(G0,[Sin*ones(length(t1),1)],t1,Y(2641,:)');
Y(2671:2971,1:3)=lsim(G1,[Sin*ones(length(t2),1)],t2,Y(2671,:)');%9 cycle
Y(2971:3001,1:3)=lsim(G0,[Sin*ones(length(t1),1)],t1,Y(2971,:)');
Y(3001:3301,1:3)=lsim(G1,[Sin*ones(length(t2),1)],t2,Y(3001,:)'); %10 cycle
subplot(2,1,1); plot(Y)
xlabel('time')
ylabel(' concentration [g/ml]')
legend('S1', 'S2','S3')
subplot(2,1,2);plot(Y(:,1:2))
xlabel('time')
ylabel(' concentration [g/ml]')
legend('S1', 'S2')
```

Appendix IX Matlab script for the selection of the optimal control strategy

```
%open loop control of the Biosep
% two intervals, three control inputs
clear
close all

Q1=0.46;
Q2=1.38;
Sin=7.97/10000;

V1=6.36;
V2=17;
V3=0.64;

k1=0.534;
k2=0.075;
k3=0.015;
k4=0.093;

Y=zeros(1e3,3,2^6);
X0=zeros(3,1);
t1=0:.1:3; t2=0:.1:30; t3=0:.1:3;
t=33 %total time of 1 cycles 33s

% systems when alpha is 1
    %1  Q1=0; Q2=0
 A1=[-k1-k2/(k4) 0 0;(V1/V2)*(k2/(k4)) 0 0; k1*V1/V3 0 0]; B1=[0;0;0];
C=eye(3); D=zeros(3,1); sys1=ss(A1,B1,C,D);
    %2 Q1=1; Q2=0
 A2=[-Q1/V1-k1-k2/(Q1+k4) 0 0;(V1/V2)*(k2/(Q1+k4)) 0 0; k1*V1/V3 0 0];
B2=[Q1/V1;0;0]; C=eye(3); D=zeros(3,1); sys2=ss(A2,B2,C,D);
    %3 Q1=0; Q2=1
 A3=[-k1-k2/(k4) 0 0;(V1/V2)*(k2/(k4)) -Q2/V2 0; k1*V1/V3 0 0];
B3=[0;Q2/V2;0]; C=eye(3); D=zeros(3,1); sys3=ss(A3,B3,C,D);
    %4 Q1=1; Q2=1
 A4=[-Q1/V1-k1-k2/(Q1+k4) 0 0;(V1/V2)*(k2/(Q1+k4)) -Q2/V2 0; k1*V1/V3 0 0];
B4=[Q1/V1;Q2/V2;0]; C=eye(3); D=zeros(3,1); sys4=ss(A4,B4,C,D);

% systems when alpha is 0
     %5 Q1=0; Q2=0
A5=[-k2/(k4) 0 k3*V3/V1;(V1/V2)*(k2/(k4)) 0 0; 0 0 -k3]; B5=[0;0;0];
C=eye(3); D=zeros(3,1); sys5=ss(A5,B5,C,D);
    %6 Q1=1; Q2=0
A6=[-Q1/V1-k2/(Q1+k4) 0 k3*V3/V1;(V1/V2)*(k2/(Q1+k4)) 0 0; 0 0 -k3];
B6=[Q1/V1;0;0]; C=eye(3); D=zeros(3,1); sys6=ss(A6,B6,C,D);
    %7 Q1=0; Q2=1
A7=[-k2/(k4) 0 k3*V3/V1;(V1/V2)*(k2/(k4)) -Q2/V2 0; 0 0 -k3];
B7=[0;Q2/V2;0]; C=eye(3); D=zeros(3,1); sys7=ss(A7,B7,C,D);
    %8 Q1=1; Q2=1
A8=[-Q1/V1-k2/(Q1+k4) 0 k3*V3/V1;(V1/V2)*(k2/(Q1+k4)) -Q2/V2 0; 0 0 -k3];
B8=[Q1/V1;Q2/V2;0]; C=eye(3); D=zeros(3,1); sys8=ss(A8,B8,C,D);

% when the short-interval has all the possible combination, and the long-
interval has only the alpha=1; Q1=0; Q2=0
Y(1:31,1:3,1)=lsim(sys1,[Sin*ones(length(t1),1)],t1,X0);
Y(31:331,1:3,1)=lsim(sys1,[Sin*ones(length(t2),1)],t2,Y(31,:,1)');
```

```
Y(1:31,1:3,2)=lsim(sys2,[Sin*ones(length(t1),1)],t1,X0);
Y(31:331,1:3,2)=lsim(sys1,[Sin*ones(length(t2),1)],t2,Y(31,:,2)');
Y(1:31,1:3,3)=lsim(sys3,[Sin*ones(length(t1),1)],t1,X0);
Y(31:331,1:3,3)=lsim(sys1,[Sin*ones(length(t2),1)],t2,Y(31,:,3)');
Y(1:31,1:3,4)=lsim(sys4,[Sin*ones(length(t1),1)],t1,X0);
Y(31:331,1:3,4)=lsim(sys1,[Sin*ones(length(t2),1)],t2,Y(31,:,4)');
Y(1:31,1:3,5)=lsim(sys5,[Sin*ones(length(t1),1)],t1,X0);
Y(31:331,1:3,5)=lsim(sys1,[Sin*ones(length(t2),1)],t2,Y(31,:,5)');
Y(1:31,1:3,6)=lsim(sys6,[Sin*ones(length(t1),1)],t1,X0);
Y(31:331,1:3,6)=lsim(sys1,[Sin*ones(length(t2),1)],t2,Y(31,:,6)');
Y(1:31,1:3,7)=lsim(sys7,[Sin*ones(length(t1),1)],t1,X0);
Y(31:331,1:3,7)=lsim(sys1,[Sin*ones(length(t2),1)],t2,Y(31,:,7)');
Y(1:31,1:3,8)=lsim(sys8,[Sin*ones(length(t1),1)],t1,X0);
Y(31:331,1:3,8)=lsim(sys1,[Sin*ones(length(t2),1)],t2,Y(31,:,8)');

% when the short-interval has all the possible combination, and the long-
interval has only the alpha=1; Q1=1; Q2=0
Y(1:31,1:3,9)=lsim(sys1,[Sin*ones(length(t1),1)],t1,X0);
Y(31:331,1:3,9)=lsim(sys2,[Sin*ones(length(t2),1)],t2,Y(31,:,9)');
Y(1:31,1:3,10)=lsim(sys2,[Sin*ones(length(t1),1)],t1,X0);
Y(31:331,1:3,10)=lsim(sys2,[Sin*ones(length(t2),1)],t2,Y(31,:,10)');
Y(1:31,1:3,11)=lsim(sys3,[Sin*ones(length(t1),1)],t1,X0);
Y(31:331,1:3,11)=lsim(sys2,[Sin*ones(length(t2),1)],t2,Y(31,:,11)');
Y(1:31,1:3,12)=lsim(sys4,[Sin*ones(length(t1),1)],t1,X0);
Y(31:331,1:3,12)=lsim(sys2,[Sin*ones(length(t2),1)],t2,Y(31,:,12)');
Y(1:31,1:3,13)=lsim(sys5,[Sin*ones(length(t1),1)],t1,X0);
Y(31:331,1:3,13)=lsim(sys2,[Sin*ones(length(t2),1)],t2,Y(31,:,13)');
Y(1:31,1:3,14)=lsim(sys6,[Sin*ones(length(t1),1)],t1,X0);
Y(31:331,1:3,14)=lsim(sys2,[Sin*ones(length(t2),1)],t2,Y(31,:,14)');
Y(1:31,1:3,15)=lsim(sys7,[Sin*ones(length(t1),1)],t1,X0);
Y(31:331,1:3,15)=lsim(sys2,[Sin*ones(length(t2),1)],t2,Y(31,:,15)');
Y(1:31,1:3,16)=lsim(sys8,[Sin*ones(length(t1),1)],t1,X0);
Y(31:331,1:3,16)=lsim(sys2,[Sin*ones(length(t2),1)],t2,Y(31,:,16)');

% when the short-interval has all the possible combination, and the long-
interval has only the alpha=1; Q1=0; Q2=1
Y(1:31,1:3,17)=lsim(sys1,[Sin*ones(length(t1),1)],t1,X0);
Y(31:331,1:3,17)=lsim(sys3,[Sin*ones(length(t2),1)],t2,Y(31,:,17)');
Y(1:31,1:3,18)=lsim(sys2,[Sin*ones(length(t1),1)],t1,X0);
Y(31:331,1:3,18)=lsim(sys3,[Sin*ones(length(t2),1)],t2,Y(31,:,18)');
Y(1:31,1:3,19)=lsim(sys3,[Sin*ones(length(t1),1)],t1,X0);
Y(31:331,1:3,19)=lsim(sys3,[Sin*ones(length(t2),1)],t2,Y(31,:,19)');
Y(1:31,1:3,20)=lsim(sys4,[Sin*ones(length(t1),1)],t1,X0);
Y(31:331,1:3,20)=lsim(sys3,[Sin*ones(length(t2),1)],t2,Y(31,:,20)');
Y(1:31,1:3,21)=lsim(sys5,[Sin*ones(length(t1),1)],t1,X0);
Y(31:331,1:3,21)=lsim(sys3,[Sin*ones(length(t2),1)],t2,Y(31,:,21)');
Y(1:31,1:3,22)=lsim(sys6,[Sin*ones(length(t1),1)],t1,X0);
Y(31:331,1:3,22)=lsim(sys3,[Sin*ones(length(t2),1)],t2,Y(31,:,22)');
Y(1:31,1:3,23)=lsim(sys7,[Sin*ones(length(t1),1)],t1,X0);
Y(31:331,1:3,23)=lsim(sys3,[Sin*ones(length(t2),1)],t2,Y(31,:,23)');
Y(1:31,1:3,24)=lsim(sys8,[Sin*ones(length(t1),1)],t1,X0);
Y(31:331,1:3,24)=lsim(sys3,[Sin*ones(length(t2),1)],t2,Y(31,:,24)');

% when the short-interval has all the possible combination, and the long-
interval has only the alpha=1; Q1=1; Q2=1
Y(1:31,1:3,25)=lsim(sys1,[Sin*ones(length(t1),1)],t1,X0);
Y(31:331,1:3,25)=lsim(sys4,[Sin*ones(length(t2),1)],t2,Y(31,:,25)');
Y(1:31,1:3,26)=lsim(sys2,[Sin*ones(length(t1),1)],t1,X0);
Y(31:331,1:3,26)=lsim(sys4,[Sin*ones(length(t2),1)],t2,Y(31,:,26)');
Y(1:31,1:3,27)=lsim(sys3,[Sin*ones(length(t1),1)],t1,X0);
Y(31:331,1:3,27)=lsim(sys4,[Sin*ones(length(t2),1)],t2,Y(31,:,27)');
```

```
Y(1:31,1:3,28)=lsim(sys4,[Sin*ones(length(t1),1)],t1,X0);
Y(31:331,1:3,28)=lsim(sys4,[Sin*ones(length(t2),1)],t2,Y(31,:,28)');
Y(1:31,1:3,29)=lsim(sys5,[Sin*ones(length(t1),1)],t1,X0);
Y(31:331,1:3,29)=lsim(sys4,[Sin*ones(length(t2),1)],t2,Y(31,:,29)');
Y(1:31,1:3,30)=lsim(sys6,[Sin*ones(length(t1),1)],t1,X0);
Y(31:331,1:3,30)=lsim(sys4,[Sin*ones(length(t2),1)],t2,Y(31,:,30)');
Y(1:31,1:3,31)=lsim(sys7,[Sin*ones(length(t1),1)],t1,X0);
Y(31:331,1:3,31)=lsim(sys4,[Sin*ones(length(t2),1)],t2,Y(31,:,31)');
Y(1:31,1:3,32)=lsim(sys8,[Sin*ones(length(t1),1)],t1,X0);
Y(31:331,1:3,32)=lsim(sys4,[Sin*ones(length(t2),1)],t2,Y(31,:,32)');

% when the short-interval has all the possible combination, and the long-
interval has only the alpha=0; Q1=0; Q2=0
Y(1:31,1:3,33)=lsim(sys1,[Sin*ones(length(t1),1)],t1,X0);
Y(31:331,1:3,33)=lsim(sys5,[Sin*ones(length(t2),1)],t2,Y(31,:,33)');
Y(1:31,1:3,34)=lsim(sys2,[Sin*ones(length(t1),1)],t1,X0);
Y(31:331,1:3,34)=lsim(sys5,[Sin*ones(length(t2),1)],t2,Y(31,:,34)');
Y(1:31,1:3,35)=lsim(sys3,[Sin*ones(length(t1),1)],t1,X0);
Y(31:331,1:3,35)=lsim(sys5,[Sin*ones(length(t2),1)],t2,Y(31,:,35)');
Y(1:31,1:3,36)=lsim(sys4,[Sin*ones(length(t1),1)],t1,X0);
Y(31:331,1:3,36)=lsim(sys5,[Sin*ones(length(t2),1)],t2,Y(31,:,36)');
Y(1:31,1:3,37)=lsim(sys5,[Sin*ones(length(t1),1)],t1,X0);
Y(31:331,1:3,37)=lsim(sys5,[Sin*ones(length(t2),1)],t2,Y(31,:,37)');
Y(1:31,1:3,38)=lsim(sys6,[Sin*ones(length(t1),1)],t1,X0);
Y(31:331,1:3,38)=lsim(sys5,[Sin*ones(length(t2),1)],t2,Y(31,:,38)');
Y(1:31,1:3,39)=lsim(sys7,[Sin*ones(length(t1),1)],t1,X0);
Y(31:331,1:3,39)=lsim(sys5,[Sin*ones(length(t2),1)],t2,Y(31,:,39)');
Y(1:31,1:3,40)=lsim(sys8,[Sin*ones(length(t1),1)],t1,X0);
Y(31:331,1:3,40)=lsim(sys5,[Sin*ones(length(t2),1)],t2,Y(31,:,40)');

% when the short-interval has all the possible combination, and the long-
interval has only the alpha=0; Q1=1; Q2=0
Y(1:31,1:3,41)=lsim(sys1,[Sin*ones(length(t1),1)],t1,X0);
Y(31:331,1:3,41)=lsim(sys6,[Sin*ones(length(t2),1)],t2,Y(31,:,41)');
Y(1:31,1:3,42)=lsim(sys2,[Sin*ones(length(t1),1)],t1,X0);
Y(31:331,1:3,42)=lsim(sys6,[Sin*ones(length(t2),1)],t2,Y(31,:,42)');
Y(1:31,1:3,43)=lsim(sys3,[Sin*ones(length(t1),1)],t1,X0);
Y(31:331,1:3,43)=lsim(sys6,[Sin*ones(length(t2),1)],t2,Y(31,:,43)');
Y(1:31,1:3,44)=lsim(sys4,[Sin*ones(length(t1),1)],t1,X0);
Y(31:331,1:3,44)=lsim(sys6,[Sin*ones(length(t2),1)],t2,Y(31,:,44)');
Y(1:31,1:3,45)=lsim(sys5,[Sin*ones(length(t1),1)],t1,X0);
Y(31:331,1:3,45)=lsim(sys6,[Sin*ones(length(t2),1)],t2,Y(31,:,45)');
Y(1:31,1:3,46)=lsim(sys6,[Sin*ones(length(t1),1)],t1,X0);
Y(31:331,1:3,46)=lsim(sys6,[Sin*ones(length(t2),1)],t2,Y(31,:,46)');
Y(1:31,1:3,47)=lsim(sys7,[Sin*ones(length(t1),1)],t1,X0);
Y(31:331,1:3,47)=lsim(sys6,[Sin*ones(length(t2),1)],t2,Y(31,:,47)');
Y(1:31,1:3,48)=lsim(sys8,[Sin*ones(length(t1),1)],t1,X0);
Y(31:331,1:3,48)=lsim(sys6,[Sin*ones(length(t2),1)],t2,Y(31,:,48)');

% when the short-interval has all the possible combination, and the long-
interval has only the alpha=0; Q1=0; Q2=1
Y(1:31,1:3,49)=lsim(sys1,[Sin*ones(length(t1),1)],t1,X0);
Y(31:331,1:3,49)=lsim(sys7,[Sin*ones(length(t2),1)],t2,Y(31,:,49)');
Y(1:31,1:3,50)=lsim(sys2,[Sin*ones(length(t1),1)],t1,X0);
Y(31:331,1:3,50)=lsim(sys7,[Sin*ones(length(t2),1)],t2,Y(31,:,50)');
Y(1:31,1:3,51)=lsim(sys3,[Sin*ones(length(t1),1)],t1,X0);
Y(31:331,1:3,51)=lsim(sys7,[Sin*ones(length(t2),1)],t2,Y(31,:,51)');
Y(1:31,1:3,52)=lsim(sys4,[Sin*ones(length(t1),1)],t1,X0);
Y(31:331,1:3,52)=lsim(sys7,[Sin*ones(length(t2),1)],t2,Y(31,:,52)');
Y(1:31,1:3,53)=lsim(sys5,[Sin*ones(length(t1),1)],t1,X0);
Y(31:331,1:3,53)=lsim(sys7,[Sin*ones(length(t2),1)],t2,Y(31,:,53)');
```

```
Y(1:31,1:3,54)=lsim(sys6,[Sin*ones(length(t1),1)],t1,X0);
Y(31:331,1:3,54)=lsim(sys7,[Sin*ones(length(t2),1)],t2,Y(31,:,54)');
Y(1:31,1:3,55)=lsim(sys7,[Sin*ones(length(t1),1)],t1,X0);
Y(31:331,1:3,55)=lsim(sys7,[Sin*ones(length(t2),1)],t2,Y(31,:,55)');
Y(1:31,1:3,56)=lsim(sys8,[Sin*ones(length(t1),1)],t1,X0);
Y(31:331,1:3,56)=lsim(sys7,[Sin*ones(length(t2),1)],t2,Y(31,:,56)');

% when the short-interval has all the possible combination, and the long-
interval has only the alpha=0; Q1=1; Q2=1
Y(1:31,1:3,57)=lsim(sys1,[Sin*ones(length(t1),1)],t1,X0);
Y(31:331,1:3,57)=lsim(sys8,[Sin*ones(length(t2),1)],t2,Y(31,:,57)');
Y(1:31,1:3,58)=lsim(sys2,[Sin*ones(length(t1),1)],t1,X0);
Y(31:331,1:3,58)=lsim(sys8,[Sin*ones(length(t2),1)],t2,Y(31,:,58)');
Y(1:31,1:3,59)=lsim(sys3,[Sin*ones(length(t1),1)],t1,X0);
Y(31:331,1:3,59)=lsim(sys8,[Sin*ones(length(t2),1)],t2,Y(31,:,59)');
Y(1:31,1:3,60)=lsim(sys4,[Sin*ones(length(t1),1)],t1,X0);
Y(31:331,1:3,60)=lsim(sys8,[Sin*ones(length(t2),1)],t2,Y(31,:,60)');
Y(1:31,1:3,61)=lsim(sys5,[Sin*ones(length(t1),1)],t1,X0);
Y(31:331,1:3,61)=lsim(sys8,[Sin*ones(length(t2),1)],t2,Y(31,:,61)');
Y(1:31,1:3,62)=lsim(sys6,[Sin*ones(length(t1),1)],t1,X0);
Y(31:331,1:3,62)=lsim(sys8,[Sin*ones(length(t2),1)],t2,Y(31,:,62)');
Y(1:31,1:3,63)=lsim(sys7,[Sin*ones(length(t1),1)],t1,X0);
Y(31:331,1:3,63)=lsim(sys8,[Sin*ones(length(t2),1)],t2,Y(31,:,63)');
Y(1:31,1:3,64)=lsim(sys8,[Sin*ones(length(t1),1)],t1,X0);
Y(31:331,1:3,64)=lsim(sys8,[Sin*ones(length(t2),1)],t2,Y(31,:,64)');

for n=1:64
    MS1(1:331,n)=Y(1:331,1,n) % the value of S1 during 1 short and 1 long
period -S1(t) for the 64 combinations;
    MS2(1:331,n)=Y(1:331,2,n);% the value of S2 during 1 short and 1 long
period -S2(t) for the 64 combinations;
end

% combination
%Q1ns- Q1, n=number of combination s-short period; l -long period;
%Q2ns- Q2, n=number of combination s-short period; l -long period:

% Qs11=0;Qs21=0;Ql11=0;Ql21=0%1st combination
Q11=zeros(331,1);
Q21=zeros(331,1);
% Qs12=1;Qs22=0;Ql12=0;Ql22=0%2nd combination
Q12=[ones(31,1);zeros(300,1)];
Q22=zeros(331,1);
% Qs13=0;Qs23=1;Ql13=0;Ql23=0%3rd combination
Q13=zeros(331,1);
Q23=[ones(31,1);zeros(300,1)];
% Qs14=1;Qs24=1;Ql14=0;Ql24=0%4th combination
Q14=[ones(31,1);zeros(300,1)];
Q24=[ones(31,1);zeros(300,1)];

% Qs15=0;Qs25=0;Ql15=1;Ql25=0%5th combination
Q15=[zeros(31,1);ones(300,1)];
Q25=zeros(331,1);
% Qs16=1;Qs26=0;Ql16=1;Ql26=0%6th combination
Q16=ones(331,1);
Q26=zeros(331,1);
% Qs17=0;Qs27=1;Ql17=1;Ql27=0%7th combination
Q17=[zeros(31,1);ones(300,1)];
Q27=[ones(31,1);zeros(300,1)];
% Qs18=1;Qs28=1;Ql18=1;Ql28=0%8th combination
Q18=ones(331,1);
```

```
Q28=[ones(31,1);zeros(300,1)];

% Qs19=0;Qs29=0;Ql19=0;Ql29=1%9th combination
Q19=zeros(331,1);
Q29=[zeros(31,1);ones(300,1)];
% Qs110=1;Qs210=0;Ql110=0;Ql210=1%10th combination
Q110=[ones(31,1);zeros(300,1)];
Q210=[zeros(31,1);ones(300,1)];
% Qs111=0;Qs211=1;Ql111=0;Ql211=1%11th combination
Q111=zeros(331,1);
Q211=ones(331,1);
% Qs112=1;Qs212=1;Ql112=0;Ql212=1%12th combination
Q112=[ones(31,1);zeros(300,1)];
Q212=ones(331,1);

% Qs113=0;Qs213=0;Ql113=1;Ql213=1%13th combination
Q113=[zeros(31,1);ones(300,1)];
Q213=[zeros(31,1);ones(300,1)];
% Qs114=1;Qs214=0;Ql114=1;Ql214=1%14th combination
Q114=ones(331,1);
Q214=[zeros(31,1);ones(300,1)];
% Qs115=0;Qs215=1;Ql115=1;Ql215=1%15th combination
Q115=[zeros(31,1);ones(300,1)];
Q215=ones(331,1);
% Qs116=1;Qs216=1;Ql116=1;Ql216=1%16th combination
Q116=ones(331,1);
Q216=ones(331,1);

% these combinations are repeated, because the short period can have
%alpha=0 or 1 and the long period, too; thus, the total combinations
% become 64
MQ11=Q1*[Q11, Q12, Q13, Q14, Q11, Q12, Q13, Q14, Q15, Q16, Q17, Q18, Q15,
Q16, Q17, Q18, Q19, Q110, Q111, Q112, Q19, Q110, Q111, Q112, Q113, Q114,
Q115, Q116, Q113, Q114, Q115, Q116 ];
MQ21=Q2*[Q21, Q22, Q23, Q24, Q21, Q22, Q23, Q24, Q25, Q26, Q27, Q28, Q25,
Q26, Q27, Q28, Q29, Q210, Q211, Q212, Q29, Q210, Q211, Q212, Q213, Q214,
Q215, Q216, Q213, Q214, Q215, Q216 ];

MQ1=[MQ11, MQ11]; % store Q1(t) for all 64 combinations
MQ2=[MQ21, MQ21]; % store Q2(t) for all 64 combinations

format short e

for n=1:64
Z1(1,n)=MS2(:,n)'*MQ2(:,n)*0.1 - MS1(:,n)'*MQ1(:,n)*0.1; % the difference
between the total mass in concentrate and filtrate solution after one
cycle; the difference should be maximal
Z2(1,n)=MS1(:,n)'*MQ1(:,n)*0.1; %total mass in filtrate solution after one
cycle; this mass should be minimal
end

figure(1)
%plot all the combinations
plot(Z1')
hold on
plot(Z2','g')
xlabel('combinations')
ylabel('total mass [g]')
legend('dm','mf')
```

```
Zf=[];
Zf(:,1)=[20,24,28,32,52,56,60,64]'; % numbers of the 8 combinations with
highest difference in total mass
Zf(:,2)=Z1([20,24,28,32,52,56,60,64])';% values of the difference in the
total mass of these 8 combinations
Zf(:,3)=Z2([20,24,28,32,52,56,60,64])'; % values of the total mass in
filtrate solution of these 8 combinations

%find out which combination has the maximal difference in the
%concentrations
[M1, I1]=max(Zf(:,1))
%find out which combination has the maximal total mass of particles
[M2, I2]=min(Zf(:,3))

figure(2)
plot(Y(1:331,1:3,[52]))
xlabel('time')
ylabel('concentration [g/ml]')
legend('S1', 'S2', 'S3')
```

Appendix X Matlab script for the simulation of the controlled BioSep

```
% Simulation of BioSep with estimated parameters
t1=0:.1:3; t2=0:0.1:30;
Sin=7.97/10000;
k1=0.534; k2=0.075; k3=10; k4=0.093;
Q1=0.46;Q2=1.38;
V1=6.36;V2=17;V3=0.64;
X0=zeros(3,1);

%alpha=1, Q1=1, Q2=1 - short period
A1=[-Q1/V1-k1-k2/(Q1+k4) 0 0;(V1/V2)*(k2/(Q1+k4)) -Q2/V2 0; k1*V1/V3 0 0]
B1=[Q1/V1;Q2/V2;0]

% alpha=0; Q1=0, Q2=1 -long period
A2 =[-k2/(k4) 0 k3*V3/V1;(V1/V2)*(k2/(k4)) -Q2/V2 0; 0 0 -k3]
B2=[0;Q2/V2;0]

C=eye(3)
D=zeros(3,1)
% creating an object G1 and G2 representing the continuous-time state-space
model;
%short period
G1=ss(A1,B1,C,D,'StateName',{'x1=S1 concentration in compartment 1';'x2=S2
concentration in compartment 2'; 'x3=S3 concentration in compartment
3'},'StateUnit',{'g/ml' ; 'g/ml'; 'g/ml'}, 'OutputName', {'y1=S1
concentration in compartment 1';'y2=S2 concentration in compartment 2';
'y3=S3 concentration in compartment 3'}, 'OutputUnit',{'g/ml' ; 'g/ml';
'g/ml'}) % when alpha=1, transducer 'on'

%long period
G2=ss(A2,B2,C,D,'StateName',{'x1=S1 concentration in compartment 1';'x2=S2
concentration in compartment 2'; 'x3=S3 concentration in compartment
3'},'StateUnit',{'g/ml' ; 'g/ml'; 'g/ml'},'OutputName', {'y1=S1
concentration in compartment 1';'y2=S2 concentration in compartment 2';
'y3=S3 concentration in compartment 3'}, 'OutputUnit',{'g/ml' ; 'g/ml';
'g/ml'})  % when alpha=0, transducer 'off'

y=[]

% simulations
Y(1:31,1:3)=lsim(G1,[Sin*ones(length(t1),1)],t1,X0);
Y(31:331,1:3)=lsim(G2,[Sin*ones(length(t2),1)],t2,Y(31,:)'); %1 cycle
Y(331:361,1:3)=lsim(G1,[Sin*ones(length(t1),1)],t1,Y(331,:)');
Y(361:661,1:3)=lsim(G2,[Sin*ones(length(t2),1)],t2,Y(361,:)');%2 cycle
Y(661:691,1:3)=lsim(G1,[Sin*ones(length(t1),1)],t1,Y(661,:)');
Y(691:991,1:3)=lsim(G2,[Sin*ones(length(t2),1)],t2,Y(691,:)');%3 cycle
Y(991:1021,1:3)=lsim(G1,[Sin*ones(length(t1),1)],t1,Y(991,:)');
Y(1021:1321,1:3)=lsim(G2,[Sin*ones(length(t2),1)],t2,Y(1021,:)');%4 cycle
Y(1321:1351,1:3)=lsim(G1,[Sin*ones(length(t1),1)],t1,Y(1321,:)');
Y(1351:1651,1:3)=lsim(G2,[Sin*ones(length(t2),1)],t2,Y(1351,:)'); %5 cycle
Y(1651:1681,1:3)=lsim(G1,[Sin*ones(length(t1),1)],t1,Y(1651,:)');
Y(1681:1981,1:3)=lsim(G2,[Sin*ones(length(t2),1)],t2,Y(1681,:)'); %6 cycle
Y(1981:2011,1:3)=lsim(G1,[Sin*ones(length(t1),1)],t1,Y(1981,:)');
Y(2011:2311,1:3)=lsim(G2,[Sin*ones(length(t2),1)],t2,Y(2011,:)');%7 cycle
Y(2311:2341,1:3)=lsim(G1,[Sin*ones(length(t1),1)],t1,Y(2311,:)');
Y(2341:2641,1:3)=lsim(G2,[Sin*ones(length(t2),1)],t2,Y(2341,:)');%8 cycle
Y(2641:2671,1:3)=lsim(G1,[Sin*ones(length(t1),1)],t1,Y(2641,:)');
Y(2671:2971,1:3)=lsim(G2,[Sin*ones(length(t2),1)],t2,Y(2671,:)');%9 cycle
```

```
Y(2971:3001,1:3)=lsim(G1,[Sin*ones(length(t1),1)],t1,Y(2971,:)');
Y(3001:3301,1:3)=lsim(G2,[Sin*ones(length(t2),1)],t2,Y(3001,:)'); %10 cycle

subplot(2,1,1); plot(Y)
xlabel('time')
ylabel(' concentration [g/ml]')
legend('S1', 'S2','S3')
subplot(2,1,2);plot(Y(:,1:2))
xlabel('time')
ylabel('concentration [g/ml]')
legend('S1', 'S2')
```